Response to Reviewer 1

Response: Thank you very much for your comments on our paper. We appreciate the time that you have taken to read our manuscript and give us your comments and suggestions. Our replies to your comments are given below in blue.

General Comments
This paper outlines air-quality evaluation of simulations conducted with the WRF-Chem model over China. Sensitivity to emissions is tested by using two commonly used anthropogenic emission inventories (REAS and EDGAR), finding large differences between the two for certain species. This is followed by an evaluation of key species relevant for air quality vs. ground site measurements across China and Japan, using output from the WRF-Chem model run with the REAS emissions.

In general, I think the paper is well written and easy to follow. However, there are several points I would like to see addressed before it would be suitable for publication. I think the paper would benefit from stronger justification (explaining the novelty of the study) and discussion of the impacts and implications of its findings. This is particularly true in the conclusions section, which mostly just summarizes the results and only offers a short last sentence of the form "These findings suggest future work is needed…"as implications of the study.

Response: Based on your helpful feedback, we have strengthened the justification for our study in the introduction and discussed the impacts and implications in the last section. We have revised the abstract, introduction, and conclusion. The newly added sentences in the revised manuscript are in Italics, as given below.

Abstract:
Our study highlights the importance of constraining emissions at the provincial level for regional air quality modeling over East Asia. Our results suggest that future work should focus on the improvement of provincial-level emissions especially estimating primary PM, SO_2 and NO_x.

Introduction section, paragraph 3 and 4:
One of the possible reasons that models underestimate particulate matter (PM) concentrations is the uncertainty in emissions. *Several emissions inventories for Asia have been developed by different groups, each with different purposes and characteristics (JRC and PBL, 2010; Kurokawa et al., 2013; Streets et al., 2003; Klimont et al., 2009). Comparison of the emissions inventories has revealed large differences in these emissions estimates. Kurokawa et al. (2013) compared different emissions inventories for several provinces in China and found that the difference in primary PM_{10} emissions can be as high as 140%. The possible causes for such discrepancies among emissions inventories are differences in estimates of: (1) activity level, (2) level of technologies implemented, and (3) emission factors. Since it is hard to measure emission factors of each individual source at the scale of a province or a country, uncertainties arise when emission factors from one place are applied to another. Activity data or emission factors are often not available at the level of detail required for making insightful comparisons across emissions inventories.*

While comparison of emissions inventories has revealed notable differences in the emissions estimates, few studies have addressed to what extent uncertainty in the emissions inventories really matter for the outcome of air quality modeling studies. Ma and van Aardenne (2004) compared simulated surface O_3 mixing ratios over China using three different emissions inventories as model inputs, and found that surface O_3 differed as much as 30–50% among different model simulations. They also demonstrated that the differences in NO_x and non-methane volatile organic compounds (NMVOCs) among different inventories were dominant factors for the discrepancies in simulated O_3 mixing ratios. Amnuaylojaroen et

al. (2014), on the other hand, studied the effect of different anthropogenic emissions inventories on air quality over Southeast Asia and found only a small difference in simulated O_3 (about 4.5 %) and CO (about 8 %) mixing ratios. However, these studies did not investigate the impact of emissions inventories on other pollutant species such as PM. *Unlike the previous studies, which focused on uncertainties of simulated O_3, CO and NO_x, this study provides quantitative information on how emissions inventories impact PM and other pollutants including SO_2.*

Conclusion section, paragraph 3:
Quantifying uncertainties of simulated air quality at the provincial level due to emission inputs reveals that the uncertainty in emissions inventories leads to significant differences in simulated levels of air pollutants, especially PM_{10}, SO_2 and NO_2. For O_3, on the contrary, different emissions inventories lead to only a moderate variability, showing agreement with the findings of previous studies (Ma and van Aardenne, 2004; Amnuaylojaroen et al. 2014). Our study highlights the importance of better constraining emissions at the provincial level for regional air quality modeling over East Asia, where anthropogenic emissions are high and air pollution is a major environmental and public health challenge. Model evaluation results also indicate that emissions inventories that do not consider local emissions control policies could result in large model discrepancies. Our results suggest that future work should focus on the improvement of provincial-level emissions especially estimating primary PM, SO_2 and NO_x.

Some more details are needed in the description of model setup for the simulations to be reproducible (details given in specific comments below).

Response: We have replied with specific comments about model setup further below and shown our replies here.

We include the aerosol-radiative feedback in our simulation. The rapid radiative transfer model (RRTM) scheme (Mlawer et al., 1997) is used to represent both shortwave and longwave radiation.

The horizontal winds, temperature, and moisture are nudged to 2007 meteorological fields at all vertical levels. The meteorological data are obtained from the National Center for Environmental Prediction (NCEP) Global Forecast System final gridded analysis datasets.

As far as I can see there is no evaluation of the meteorology in the model in the paper. Representing the meteorology reasonably is a first-order pre-requisite for simulating the air-quality accurately. Please show some comparisons of key meteorological variables with some ground sites and/or satellite products (e.g. TRMM), either in the main paper or supplementary material.

Response: We have added comparisons of modeled and observed 2 m temperature, 2 m relative humidity, and 10 m wind speed in Table S4 in the supplementary material and inserted the following text in the main paper, section 4, paragraph 2.

Before evaluating the model performance in simulating air pollutants, we evaluate the simulated meteorological fields, including daily mean 2 m temperature, 2 m relative humidity, and 10 m wind speed against observations from National Climate Data Center of China Meteorological Administration for year 2007 (Table S4). The model reproduces 2 m temperature with a correlation of 0.97 and a negative NMB of -14.57 %. Relative humidity is simulated with a correlation of 0.71 and a positive NMB of 7.02 %. Compared to temperature and relative humidity, the 10 m wind speed has a relatively lower correlation of 0.52 and a higher positive NMB of 59.35 %. Overall, the model performance in simulating these meteorological data is similar to that reported for regional air quality models (Zhang et al., 2015; Tuccella 2012; Tessum et al., 2015).

Table S4 reads as follows:

Table S4. Statistical performance of WRF-Chem-REAS simulations for meteorology. Daily meteorological observations at 194 stations in 2007 are obtained from the website of National Climate Data Center of China Meteorological Administration (http://data.cma.cn/).

Meteorological items	Count	Obs.	Model	r	MB	ME	NMB	NMSE
2 m temperature (degree C)	23841	11.51	9.83	0.97	-1.68	2.43	-14.57	0.1
2 m relative humidity (%)	23862	61.77	66.1	0.71	4.34	12.34	7.02	0.06
10 m wind speed (m/s)	23857	2.18	3.48	0.52	1.29	1.49	59.35	0.47

In section 4, there is no evaluation of $PM_{2.5}$ against measurements. I appreciate that for section 3, this is not possible for the emissions sensitivity comparison without $PM_{2.5}$ emissions in EDGAR. However, this is not a limitation in the later half of the paper, where you are just using the REAS case study. It looks as though the PM_{10} results you present are being strongly impacted by dust (given the highest readings are in the North West), so looking at $PM_{2.5}$ should be more representative of anthropogenic pollution. Amalgamating $PM_{2.5}$ comparisons into section 4.1 as a single PM section would be beneficial.

Response: We appreciate your comment; however we are unable to evaluate $PM_{2.5}$ against measurements for 2007 since $PM_{2.5}$ measurement in China started in late 2012. We are working on a model evaluation paper focused on 2013, which will include extensive $PM_{2.5}$ observations. We have added the following text in section 2.3, paragraph 2.

We are unable to evaluate $PM_{2.5}$ against measurements for 2007 since $PM_{2.5}$ measurements in China started in late 2012.

Specific comments

1. Pg 9377, ln 11-13: You should not be presenting your findings in the introduction. Replace this sentence with a reference which says supports your statement, i.e. which highlights the variation in PM emissions between inventories and the uncertainties in emission estimates.

Response: We agree with the reviewer and have replaced our findings with a reference in section 1, paragraph 3. It reads as follows:

Several emissions inventories for Asia have been developed by different groups, each with different purposes and characteristics (JRC and PBL, 2010; Kurokawa et al., 2013; Streets et al., 2003; Klimont et al., 2009). Comparison of the emissions inventories has revealed large differences in these emission estimates. Kurokawa et al. (2013) compared different emissions inventories for several provinces in China and found that the difference in primary PM_{10} emissions can be as high as 140%.

2. Pg 9377, ln 23-24: Are there really no other studies investigating PM dependence to emissions inventory in Asia?

Response: To the best of our knowledge, all references we found are discussing the influence of emissions inventories on gaseous pollutants. We would be grateful if the reviewer could point us to such studies that we might have missed.

3. Pg9378, ln 10: Zhang et al., 2015 is at least one paper I know of which compares WRF-Chem model output with a wide array of measurements across China (albeit mostly just for PM2.5). As one of the main justifications of your study was that it is the first WRF-Chem study to compare against an extensive

network in East Asia, please expand on why your study is novel in light of this (and possibly other) papers.

Response: We agree that extensive $PM_{2.5}$ observations were used to evaluate WRF-Chem simulations by Zhang et al. (2015), albeit all the measurements were for time period beginning late 2012. However, our focus is 2007, when $PM_{2.5}$ in China was not available. There are a few studies that use a large array of historical PM_{10} for WRF-Chem study. In addition to PM_{10}, we also compare other gaseous pollutants such as O_3, SO_2 and NO_2. We compare data not only in China but also in Japan and Nepal and investigate the seasonal variability of each pollutant, which has not been performed previously.

Section 2.1: some questions on model setup:

4. Do you run with aerosol-radiative feedback?

Response: Yes, we include aerosol-radiative feedback in our model setup. We have included the following descriptions in Section 2.1, paragraph 1.

We include the aerosol-radiative feedback in our simulation. The rapid radiative transfer model (RRTM) scheme (Mlawer et al., 1997) is used to represent both shortwave and longwave radiation.

5. Do you periodically re-initiate the meteorology, or run with nudged met?

Response: We run the model with nudged meteorology. The following description has been added in section 2.1, paragraph 1.

The horizontal winds, temperature, and moisture are nudged to 2007 meteorological fields at all vertical levels. The meteorological data are obtained from the National Center for Environmental Prediction (NCEP) Global Forecast System final gridded analysis datasets.

6. Do you know how sensitive your model simulations are to the boundary conditions? It seems as though you are using 2010 data from AM3, is that representative of the 2007 period you are running over? Is there any reason why you are not using a product driven by meteorological reanalysis, e.g. MOZART-4 (Emmons et al., 2010)?

Response: We performed an additional simulation in July 2007 with boundary conditions obtained from MOZART-4 for year 2007. The comparisons of simulated PM_{10}, O_3, NO_2 and SO_2 using two different boundary conditions are shown in Table 1 below. We find that the boundary conditions have a small influence on simulated monthly mean O_3 and NO_2 mixing ratios. For these two pollutants, 2007 MOZART-4 boundary leads to lower MFB and NMB, while 2010 AM3 shows a stronger correlation. Based on this analysis we conclude that our model-simulated pollutant concentrations are not significantly sensitive to boundary conditions.

Table 1. Statistical measures calculated from two simulations using 2010 AM3 and 2007 MOZART-4 as boundary inputs.

Pollutants	Boundary	Obs.	Model	r	NMB	MFB	MFE	NMSE
PM_{10}	2010 AM3	82.45	80.40	0.37	-2.49	-9.86	48.13	0.36
	2007 MOZART	82.45	79.02	0.39	-4.16	-13.70	50.72	0.38
O_3	2010 AM3	35.18	43.58	0.78	23.87	25.98	30.16	0.10
	2007 MOZART	35.18	39.29	0.64	11.68	15.20	29.28	0.11
SO_2	2010 AM3	4.82	8.25	0.74	71.14	30.77	74.02	1.90
	2007 MOZART	4.82	8.74	0.73	81.35	42.71	77.11	1.99
NO_2	2010 AM3	17.54	12.17	0.73	-30.60	-54.99	62.01	0.47
	2007 MOZART	17.54	13.24	0.63	-24.50	-27.61	49.97	0.51

7. Pg 9380, section 2.2: Do you have any seasonal or diurnal variation in your emissions? If not, you should also mention this when discussing potential reasons for model discrepancy, particularly in terms of different magnitudes of error in different seasons in section 4.

Response: REAS emissions are monthly, while EDGAR emissions are yearly. We considered diurnal variation when we processed the emissions. We have added the following description of seasonal and diurnal variation in section 2.2, paragraph 2:

We apply the same diurnal variation to both REAS and EDGAR. REAS emissions inventory provides monthly emissions for each pollutant, while the EDGAR emissions inventory only provides yearly emissions estimates.

8. Pg 9381 ln 25 – pg 9382 ln 3: The sentence "For PM10, we use the performance goals and criteria of Boylan and Russell (2006)." Is redundant. Please delete and put the reference at the start of the next sentence :" Following Boylan and Russell (2006), we set…"

Response: We agree with the reviewer and made changes according to the comments above in section 2.4, paragraph 1.

Following Boylan and Russell (2006), we set the performance goals of PM_{10} as: MFB less than or equal to ± 30 % and MFE less than or equal to 50 %. The performance criteria of PM_{10} are MFB ≤ ± 60 % and MFE ≤ 75 %.

9. When you say "…goals and criteria for MFB to be less than or equal to 30 and 60%, respectively", it is not clear what the ±30% and ±60% refer to, as you are only discussing MFB for PM10. Please clarify.

Response: We have rewritten the sentence as follows:

Following Boylan and Russell (2006), we set the performance goals of PM_{10} as: MFB less than or equal to ± 30 % and MFE less than or equal to 50 %. The performance criteria of PM_{10} are MFB ≤ ± 60 % and MFE ≤ 75 %.

10. Add "±" in front of "50%", "75%" and "35%".

Response: These numbers are for mean fractional error (MFE), which is always positive.

$$MFE = \frac{1}{n}\sum_{i=1}^{n}\frac{2|Mi - Oi|}{Mi + Oi} \times 100\%$$

11. Pg 9382 ln 13: Please make explicitly clear here that the similarity in SO_2 emissions is purely coincidental, and you would probably get very different values if the domain was different.

Response: We agree with the reviewer and have added the following sentence in the revised manuscript, section 3.1, paragraph 1.

We note that this similarity is purely coincidental and depends on the domain. In certain parts of the domain REAS estimate is higher than EDGAR, while the opposite is true for other parts of the domain. When averaged over the whole domain, both inventories produce similar estimates (Fig. 2).

12. Pg 9383 ln 4-5: While I appreciate doing a detailed analysis on the causes of differences in emissions between inventories is out of the scope of the paper, it would be interesting to have some more detail on why the two are different. This discussion may be better placed in the introduction or section 2.2 than here.

Response: We have added more detail on the cause of uncertainties in different emissions inventories in section 1, paragraph 3.

The possible causes for such discrepancies among emissions inventories are differences in estimates of: (1) activity level, (2) level of technologies implemented, and (3) emission factors. Since it is hard to measure emission factors of each individual source at the scale of a province or a country, uncertainties arise when emission factors from one place are applied to another. Activity data or emission factors are often not available at the level of detail required for making insightful comparisons across emissions inventories.

13. Pg 9383 ln 22: change "large" to "largest".

Response: Corrected.

14. Pg 9383 ln 3-4: It would be helpful for those with less knowledge of the geography of China to have a visual representation of the different Chinese regions, rather than just a list in the supplement. Perhaps boxes drawn over the different regions in Fig. 1, or a similar map in the supplementary material?

Response: We have added a supplemental figure, Fig. S1, to highlight the geographic location of each region.

Figure S1. The seven regions in mainland China used for analysis in this paper.

15. pg 9384, ln 11: I am confused by the line "More detailed comparisons, assessing the impacts due to various inventories, will be conducted in our future work." This stuck me as a strange way to structure a set of papers. I agree that having more emission inventories to compare would be of benefit, but I would have thought the best place to present that would be in this paper, rather than another one. This would make the emissions sensitivity section much more interesting. A second paper focused on a more thorough evaluation with the chosen inventory (REAS) and/or investigating other scientific questions (e.g. impacts on health/climate) would make an interesting follow up. Please comment as to why you have written the papers in this form.

Response: We have deleted this sentence. We thank the reviewer for suggestions on how to construct a set of papers, which we hope to adopt in the future.

16. Pg 9385, ln 24-25. I see you have measurements from Lhasa, please can you comment on whether your modelled seasonal trends of PM_{10} in Tibet are seen in the measurements as well. If they diverge, what does this say about the dust emission scheme?

Response: The following table compares monthly mean observed and modeled PM_{10} from Lhasa. In terms of the trend, the modeled PM_{10} agrees with the observations, with the highest value in January, followed by April, October, and July. In April, July, and October, the model underestimates 50-60 % of the measurement.

Table 2. Comparison between observed and modeled monthly mean PM_{10} concentration at Lhasa, Tibet.

PM_{10} ($\mu g/m^3$)	January	April	July	October
Observed	102	82	55	68
Modeled	116	40	24	27

17. Pg 9386, ln 15-17. This can be evaluated by comparing the wintertime model meteorology with measurements.

Response: We further compared the simulated and observed wind speed in four months of 2007 and found that wind speed in the winter tends to be overestimated as shown in the following Table 3. This result illustrates that WRF-Chem has difficulties simulating stagnant conditions in winter.

Table 3. Statistical measures calculated from REAS drived simulations for wind speed.

Month	Obs.	Model	r	MB	ME	NMB	NMSE
Jan.	1.97	3.38	0.49	1.41	1.59	71.40	0.62
Apr.	2.55	3.88	0.56	1.33	1.53	52.13	0.37
Jul.	2.13	3.24	0.39	1.11	1.34	51.97	0.41
Oct.	2.08	3.42	0.57	1.34	1.51	64.04	0.51

18. Pg 9388, ln 2-3. Please comment on the seasonal variation of your emissions in the model. If there is none, the difference in modeled concentrations must be due to meteorological changes between the seasons.

Response: We have checked the monthly emissions of SO_2 in China, as shown in the following Table 4, and realized that January is not the highest emission month among the four, although the simulated SO_2 mixing ratio is the highest. We agree with the reviewer that the modeled difference in SO_2 concentrations is mostly due to meteorological changes between the seasons. We have deleted the previous discussion on emissions.

Table 4. Monthly total SO_2 (kt/month) emissions in China.

January	April	July	October
2872	2686	2883	2898

19. Table 3, 4, 5 and 6. Please say in the caption that you are using data from the WRFChem-REAS simulation. I know you say this in the text, but it is good to be reminded here to avoid confusion.

Response: We have made changes accordingly.

20. Figures 4, 7, 9 and 10. These figures will look clearer if lowest value of the scale is set to the first value above 0 (e.g. 20 instead of 0 for figure 4), as this will make the background white and make it easier to pick out regions of higher loadings .

Response: We have created figures based on the reviewer's suggestion, as seen below. However, after comparing those with our original figures, we still prefer the latter since regions in white background appear as if there are missing values.
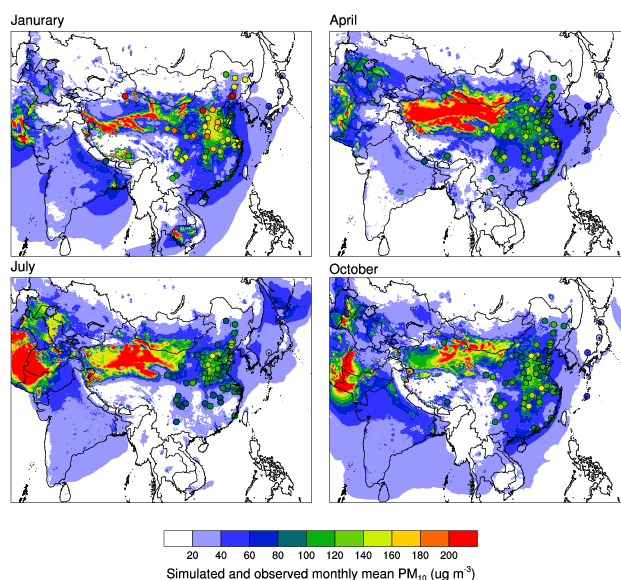
Figure 4. Simulated and observed monthly average surface PM$_{10}$ in 2007 using WRF-Chem-REAS. The filled circles indicate the observed monthly average values

References

Emmons, L. K., Walters, S., Hess, P. G., Lamarque, J.-F., Pfister, G. G., Fillmore, D., Granier, C., Guenther, A., Kinnison, D., Laepple, T., Orlando, J., Tie, X., Tyndall, G., Wiedinmyer, C., Baughcum, S. L. and Kloster, S.: Description and evaluation of the Model for Ozone and Related chemical Tracers, version 4 (MOZART-4), Geosci. Model Dev., 3(1), 43–67, doi:10.5194/gmd-3-43-2010, 2010.

Zhang, B., Wang, Y. and Hao, J.: Simulating aerosol–radiation–cloud feedbacks on meteorology and air quality over eastern China under severe haze conditions in winter, Atmos. Chem. Phys., 15, 2387–2404, doi:10.5194/acp-15-2387-2015, 2015.

Response to Reviewer 2

Thank you very much for your comments on our paper. We appreciate the time that you have taken to read our manuscript and give us your comments and suggestions. Our replies to your comments are given below in blue.

Anonymous Referee #2
General comments:
This research presented the WRF-Chem model evaluation over East and South Asia. For model evaluations, the authors uses EANET observation network, Kathmandu valley site, Mt Lulin site in Taiwan. Moreover, API was used as a proxy of PM10 concentration in China. Such synergetic analysis over Asia, where the air quality is concerned issue, are needed to further promote our understanding. Before the model evaluation, the authors provided the sensitivity simulations on the basis of two different emission inventories of REAS and EDGAR. This is also the attractive point of this study. However, some discussion points would not be robust. I would like to recommend the authors to revise the manuscript.

Response: We thank reviewer 2 for the positive comments. We have revised the manuscript based on your suggestions.

1) 'South Asia' is included in the title of this manuscript, and discussed (P9386. L17-25). However, the model evaluation was done at only one site of Kathmandu valley and for only PM10. It would not be appropriate to include 'South' in title of this manuscript. Are there no observation dataset as network or literature over India or any other countries in South or Southeast Asia?

Response: In this manuscript, we are focusing on the observation dataset in China and thus we have taken out "South Asia" from the title as suggested.

2) The concluding remarks of 'The findings suggest that future model development and evaluation of emission inventories and models are needed for particulate matter and gaseous pollutants in East and South Asia' on Abstract and Conclusions section is general and ambiguous. This sentence will not provide the authors findings through this study.

Response: We have expanded on this sentence and changed the abstract and conclusion as follows:

Abstract:
Our study highlights the importance of constraining emissions at the provincial level for regional air quality modeling over East Asia. Our results suggest that future work should focus on the improvement of provincial-level emissions especially estimating primary PM, SO_2 and NO_x.

Conclusion section, paragraph 3:
Quantifying uncertainties of simulated air quality at the provincial level due to emission inputs reveals that the uncertainty in emissions inventories leads to significant differences in simulated levels of air pollutants, especially PM_{10}, SO_2 and NO_2. For O_3, on the contrary, different emissions inventories lead to only a moderate variability, showing agreement with the findings of previous studies (Ma and van Aardenne, 2004; Amnuaylojaroen et al. 2014). Our study highlights the importance of better constraining emissions at the provincial level for regional air quality modeling over East Asia, where anthropogenic emissions are high and air pollution is a major environmental and public health challenge. Model evaluation results also indicate that emissions inventories that do not consider local emissions control

policies could result in large model discrepancies. Our results suggest that future work should focus on the improvement of provincial-level emissions especially estimating primary PM, SO$_2$ and NO$_x$.

3) Discussion on the sensitivity simulation with different two emissions of REAS and EDGAR will not be robust. The authors concluded that the REAS inventory showed better performance, and the further study was conducted with REAS. However, this conclusion was simply from the sensitivity simulation on the 14-day simulation in July 2007. What about other period? At least, I recommend the authors to provide the specific reason to select this 14-day simulation to evaluate two different inventories.

Response: The purpose of the 14-day simulation in July 2007 was to show that the REAS simulation exhibited a smaller discrepancy between observed and simulated data than the EDGAR simulation did. For a different study, we conducted simulations in 2008, January and July, using REAS and EDGAR inventories. Therefore, we have compared these model simulations with 2007 observations since we do not have 2008 observational data. The comparison is shown in the following table. We find that the REAS simulation has less bias and less error than the EDGAR simulation in January and July for PM$_{10}$ and NO$_2$, while EDGAR has slightly less bias and error for SO$_2$ only in January in terms of NMB and MFB. EDGAR and REAS simulations are similar for reproducing O$_3$. These two-month comparisons agree with what we find using 14-day simulation in July. This is why we argue that a 14-day simulation is able to represent other periods.

We add the following sentence in section 3.2, paragraph 2 in the revised manuscript to justify the use of 14-day simulation.

We have conducted additional sensitivity simulations using REAS and EDGAR in January and July and compared the simulated air pollutants and observation. The results of these two-month simulations (not shown here) agree with what we find here.

Table 1: Statistical measures for REAS and EDGAR simulations in January and July.

Pollutants	month	REAS					EDGAR				
		r	NMB	MFB	MFE	NMSE	*r*	NMB	MFB	MFE	NMSE
PM$_{10}$	Jan	0.07	-17.92	-24.12	62.61	0.81	0.02	-47.15	-59.86	77.89	1.34
	Jul	0.29	-11.64	-23.58	57.97	0.47	0.18	-47.56	-64.25	75.47	0.91
O$_3$	Jan	0.24	19.75	20.58	25.71	0.09	0.34	22.03	22.51	26.49	0.09
	Jul	0.43	19.21	18.20	36.50	0.20	0.41	21.85	21.53	36.91	0.21
SO$_2$	Jan	0.52	-18.78	-20.19	77.79	1.84	0.55	-0.35	6.34	71.52	1.51
	Jul	0.55	64.43	42.18	95.89	1.97	0.43	93.60	69.15	103.28	2.63
NO$_2$	Jan	0.40	-31.33	-43.21	59.63	0.56	0.31	-45.89	-58.88	69.14	0.87
	Jul	0.59	-26.18	-23.25	60.81	0.47	0.52	-52.46	-59.20	82.80	1.20

Specific comments:
4) P9377, L9-11: Does this sentence refer the finding from this study or other study? If the former, it should not be mention here. If the latter, please insert the appropriate references.

Response: This is the finding from this study. We have revised this sentence and added the following text in section 1, paragraph 3. It reads as follows:

Several emissions inventories for Asia have been developed by different groups, each with different purposes and characteristics (JRC and PBL, 2010; Kurokawa et al., 2013; Streets et al., 2003; Klimont et al., 2009). Comparison of the emissions inventories has revealed large differences in these emission

estimates. Kurokawa et al. (2013) compared different emissions inventories for several provinces in China and found that the difference in primary PM_{10} emissions can be as high as 140%.

5) P9378, L9-12: What is the necessity to use WRF-Chem model? What are the advantages?

Response: We have added the following sentences to explain the advantages of using WRF-Chem in Section 1, paragraph 5.

WRF-Chem is an online-coupled meteorology and chemistry model, simulating meteorological quantities and air pollution concentrations simultaneously and allowing two-way interactions between meteorological and chemical constituents. In regions with high PM loading, meteorology-chemistry interaction significantly improves model performance in simulating air pollutant concentrations. (Kong et al. 2015)

6) P9378, L21: Was the aerosol-radiation feedback tuned on in the WRF-Chem simulation?

Response: Yes, we include aerosol-radiative feedback in our model setup. We have included the following descriptions in Section 2.1, paragraph 1.

We include the aerosol-radiative feedback in our simulation. The rapid radiative transfer model (RRTM) scheme (Mlawer et al., 1997) is used to represent both shortwave and longwave radiation.

7) P9379, L13-21: Why the lateral boundary condition was not corresponded to analyzed period?

Response: We performed an additional simulation in July 2007 with boundary conditions obtained from MOZART-4 for year 2007. The comparisons of simulated PM_{10}, O_3, NO_2 and SO_2 using two different boundary conditions are shown in Table 2 below. We find that the boundary conditions have a small influence on simulated monthly mean O_3 and NO_2 mixing ratios. For these two pollutants, 2007 MOZART-4 boundary leads to lower MFB and NMB, while 2010 AM3 shows a stronger correlation. Based on this analysis we conclude that our model simulated pollutant concentrations are not significantly sensitive to boundary conditions.

Table 2. Statistical measures calculated from two simulations using 2010 AM3 and 2007 MOZART-4 as boundary inputs.

Pollutants	Boundary	Obs	Model	r	NMB	MFB	MFE	NMSE
PM_{10}	2010 AM3	82.45	80.40	0.37	-2.49	-9.86	48.13	0.36
	2007 MOZART	82.45	79.02	0.39	-4.16	-13.70	50.72	0.38
O_3	2010 AM3	35.18	43.58	0.78	23.87	25.98	30.16	0.10
	2007 MOZART	35.18	39.29	0.64	11.68	15.20	29.28	0.11
SO_2	2010 AM3	4.82	8.25	0.74	71.14	30.77	74.02	1.90
	2007 MOZART	4.82	8.74	0.73	81.35	42.71	77.11	1.99
NO_2	2010 AM3	17.54	12.17	0.73	-30.60	-54.99	62.01	0.47
	2007 MOZART	17.54	13.24	0.63	-24.50	-27.61	49.97	0.51

8) P9380, L3: Does 'PM_{10}' in emissions (shown in Table 1 and Fig. 2) include PM2.5? Also, '$PM_{2.5}$' in emissions include BC, OC, and other primary particulate matter which aerodynamic diameter less than 2.5 micrometer?

Response: Yes, PM_{10} emissions in Table 1 and Fig. 2 include all primary particulate matter with an aerodynamic diameter of less than 10μm. $PM_{2.5}$ emissions from REAS include BC, OC, and other species.

9) P9380, L17-19: So, what is the treatment of BC, OC, and PM2.5 on the simulation using EDGAR? Taken from REAS?

Response: For the simulation using EDGAR, we only read PM_{10} emissions as provided by EDGAR, which include BC, OC, and other unspeciated primary $PM_{2.5}$ and coarse PM_{10}. We did not add additional BC, OC, and $PM_{2.5}$ from other emissions inventories. We have conducted a sensitivity simulation where PM_{10} of EDGAR was split to each species as mentioned above, using weight factors calculated from REAS. The results are provided in Table 5 below. As you can see, they do not affect our simulation results and conclusions of this paper.

Table 5. Comparisons of statistic measures for simulations using EDGAR inputs with and without decoupled PM_{10}

Treatment of PM_{10}	r	NMB	MFB	MFE	NMSE
BC, OC, $PM_{2.5}$, coarse PM_{10} (sensitivity simulation)	0.15	-32.82	-45.93	64.20	0.72
Total PM_{10} (original)	0.20	-27.28	-37.34	56.70	0.58

10) P9380, L22: Please specify the temporal resolution (e.g., hourly, daily, monthly, annual) on each emission inventory used in this study.

Response: REAS emissions are monthly, while EDGAR emissions are yearly. We considered diurnal variation when we processed the emissions. We have included the description of seasonal and diurnal variation in section 2.2 paragraph 2. It reads as:

We apply the same diurnal variation to both REAS and EDGAR. REAS emissions inventory provides monthly emissions for each pollutant, while the EDGAR emissions inventory provides only yearly emissions estimates.

11) P9386, L14-17: However, better performance in weather will be the advantage of the 'online' coupled WRF-Chem model compared to other model (e.g., CMAQ).

Response: We agree with the reviewer that online coupled model is better than 'offline' models in simulating meteorology. However, as reported by many other studies, WRF-Chem still has difficulties in simulating stagnant weather conditions. We further compared the simulated and observed wind speed in four months of 2007 and found that wind speed in the winter tends to be overestimated, as shown in Table 6. This result illustrates that WRF-Chem also has difficulties simulating stagnant conditions in winter.

Table 6. Statistic measures for wind speed in different months.

Month	Obs.	Model	r	MB	ME	NMB	NMSE
Jan	1.97	3.38	0.49	1.41	1.59	71.40	0.62
Apr	2.55	3.88	0.56	1.33	1.53	52.13	0.37
Jul	2.13	3.24	0.39	1.11	1.34	51.97	0.41
Oct	2.08	3.42	0.57	1.34	1.51	64.04	0.51

12) P9387, L13-15: But Happo in Japan is also mountainous site (Table S2b). Any other reasons?

Response: The reviewer is correct that both Happo (2860m) and Lulin (1850m) are mountainous sites. However, ozone levels at these two sites are very different. The 4-month average O_3 is 60ppbv at Happo and 32 ppbv at Lulin. Our model largely overestimates O_3 at Lulin in October as shown in the table below. As suggested by the study of Ou Yang et al (2012), Lulin has more pronounced mountain valley circulation in the fall, which leads to low O_3 mixing ratios in October. Due to our model resolution, WRF-Chem is not able to capture such local meteorological characteristics. We have included Table S7 in supporting material and added the following text in section 4.2, paragraph 2. It reads as:

Statistical analysis of O_3 in different seasons at the Lulin site (Table S7) reveals that such high bias is mainly caused by overestimation in October (MFB = 63 %). A previous study by Ou Yang et al (2012) suggested that Lulin has more pronounced mountain valley circulation in fall, which leads to low observed O_3 mixing ratios in October. Our model with a horizontal resolution of 20 km x 20 km is not able to capture such local meteorology.

Table S7. Statistical measures for O_3 at the Lulin site in different months.

month	Obs.	Model	r	NMB	MFB	MFE	NMSE
Jan	32.97	48.39	0.63	46.80	37.99	37.99	0.17
Apr	50.80	53.40	0.38	5.11	4.95	17.63	0.05
Jul	21.14	35.16	0.48	66.35	49.60	49.60	0.33
Oct	23.40	44.42	0.35	89.84	62.80	62.92	0.51

Additionally, while analyzing O_3 in Lulin, we realized an error in reading the data in January at this site. We have corrected Tables 4 and S6 and Figures 7 and 8, which used O_3 data in January in Lulin. This correction does not affect our previous findings and discussion.

13) P9388, L2-4: What is the source of coal combustion?

Response: We checked the monthly emissions of SO_2 in China in January, and realized that this is not the highest emission month among the four. We have deleted the sentence about coal combustion.

14) P9390, L7: Correct the typo 'mode'.

Response: Corrected.

15) Figures 8 and 11: X-axis have different months, so these figures have some difficulty to understand.

Response: Based on the suggestion, we have added grey lines between months in the figures. Figures 8 and 11 have been updated as shown below.
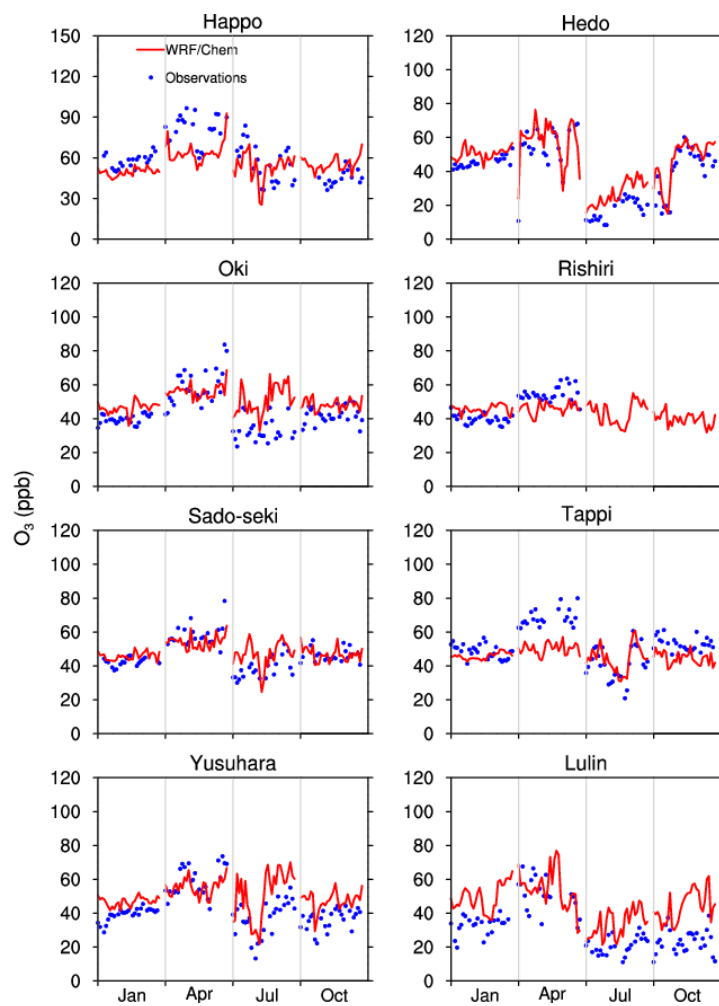
Figure 8. Comparisons of observed (blue dots) and modeled (red lines) daily mean O_3 (ppbv) at seven sites in Japan and one site in Taiwan.
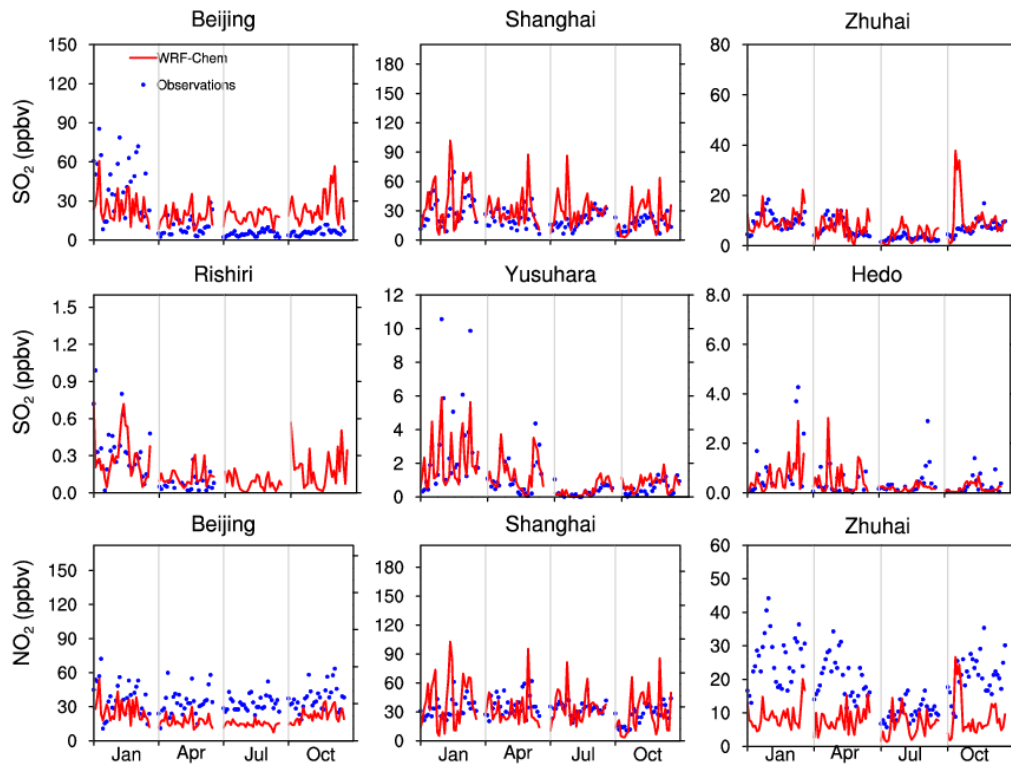
Figure 11. Comparisons of observed (blue dots) and modeled (red lines) daily mean SO_2 (ppbv) at six sites in China and Japan and NO_2 (ppbv) at three sites in China.

Air Quality Modeling with WRF-Chem v3.5 in East Asia: Sensitivity to Emissions and Evaluation of Simulated Air Quality

M. Zhong[1], E. Saikawa[1,2], Y. Liu[2], V. Naik[3,4], L. W. Horowitz[3], M. Takigawa[5], Y. Zhao[6], N.-H. Lin[7], and E. A. Stone[8]

[1]Department of Environmental Sciences, Emory University, Atlanta, GA, USA
[2]Department of Environmental Health, Rollins School of Public Health, Emory University, Atlanta, GA, USA
[3]NOAA Geophysical Fluid Dynamics Laboratory, Princeton, NJ, USA
[4]University Corporation for Atmospheric Research, Boulder, CO, USA
[5]Japan Agency for Marine-Earth Science and Technology, Yokohama, Japan
[6]Nanjing University, Nanjing, China
[7]Department of Atmospheric Sciences, National Central University, Chuang-Li, Taiwan
[8]Department of Chemistry, University of Iowa, Iowa City, IA, USA

Correspondence to: M. Zhong (min.zhong@emory.edu), E. Saikawa (eri.saikawa@emory.edu)

Abstract. We conducted simulations using the Weather Research and Forecasting model coupled with Chemistry (WRF-Chem) version 3.5 to study air quality in East Asia at a spatial resolution of 20 km $\times$ 20 km. We find large discrepancies between two existing emissions inventories: the Regional Emission Inventory in Asia version 2 (REAS) and the Emissions Database for Global Atmospheric

5   Research version 4.2 (EDGAR) at the provincial level in China, with maximum differences of up to 500 % for CO emissions, 190 % for NO, and 160 % for primary PM_{10}. Such differences in the magnitude and the spatial distribution of emissions for various species lead to 40–70 % difference in surface PM_{10} concentrations, 16–20 % in surface O_3 mixing ratios, and over 100 % in SO_2 and NO_2 mixing ratios in the polluted areas of China. WRF-Chem is sensitive to emissions, with

10   the REAS-based simulation reproducing observed concentrations and mixing ratios better than the EDGAR-based simulation for July 2007. We conduct additional model simulations using REAS emissions for January, April, July, and October of 2007 and evaluate simulations with available ground-level observations. The model results illustrate clear regional variations in the seasonal cycle of surface PM_{10} and O_3 over East Asia. The model meets the air quality model performance criteria

15   for both PM_{10} (mean fractional bias, MFB $\leqslant \pm 60$ %) and O_3 (MFB $\leqslant \pm 15$ %) in most of the observation sites, although the model underestimates PM_{10} over Northeast China in January. The model predicts the observed SO_2 well at sites in Japan, while it tends to overestimate SO_2 in China in July and October. The model underestimates observed NO_2 in all four months. *Our study highlights the importance of constraining emissions at the provincial level for regional air quality modeling*

over East Asia. Our results suggest that future work should focus on the improvement of provincial-level emissions especially estimating primary PM, SO_2 *and* NO_x.

1 Introduction

Many Asian countries have faced deteriorating air quality since the late 1990s and early 2000s due to rapid economic development and population growth. According to the latest World Health Organization (WHO) ambient air pollution database (WHO, 2014) , air quality in China and India were ranked 14th and 9th respectively, out of the 91 most polluted countries. Since these countries have the largest population in the world, exposure to air pollutants poses health risks to billions of residents. For example, Chen et al. (2013) reported that outdoor air pollution in China alone caused approximately half a million premature deaths every year. A similar number of premature deaths was estimated in India in 2010 (HEI, 2013). Air pollution not only impacts human health, but also has important potential consequences for natural ecosystems, crop yields, visibility, and radiative forcing (Seinfeld and Pandis, 2012). In order to mitigate these negative consequences, it is essential to have a better understanding of air pollutant emissions sources and magnitudes, as well as atmospheric transport and chemical composition over the region.

Several modeling studies have applied the Weather Research and Forecasting model coupled with Chemistry (WRF-Chem) (Grell et al., 2005) to study air quality in Asia. Saikawa et al. (2011) analyzed the impact of China's vehicle emissions on air quality both within China and across East Asia. They found that stricter regulation of the road transport sector in China would reduce surface concentrations of fine particulate matter with an aerodynamic diameter of 2.5μm or less ($PM_{2.5}$) and tropospheric ozone (O_3) mixing ratios in the region. Kumar et al. (2012) examined ground level measurements and satellite observations in South Asia and reported that WRF-Chem could simulate O_3 and CO well but large discrepancies were found for NO_2 due to uncertainties in emissions from biomass burning and anthropogenic NO_x estimates. Wang et al. (2010) conducted sensitivity analyses of O_3, NO_x, and sulfur dioxide (SO_2) mixing ratios to temporal and vertical emissions; their results showed that air quality in East Asia was impacted by the diurnal and vertical distribution of anthropogenic emissions. Studies that have conducted WRF-Chem modeling for $PM_{2.5}$ and PM_{10} have found that these surface concentrations were usually underestimated. For example, Saikawa et al. (2011) reported that modeled four-month average $PM_{2.5}$ concentrations at Oki and Rishiri in Japan had a mean normalized bias (MNB) of -34 % compared to observations. Gao et al. (2014) compared simulated and measured PM_{10} concentrations at six sites in Japan and found that the model underestimated the annual average PM_{10} at all sites except one.

One of the possible reasons that models underestimate particulate matter (PM) concentrations is the uncertainty in emissions. *Several emissions inventories for Asia have been developed by different groups, each with different purposes and characteristics (Kurokawa et al., 2013; JRC and*

PBL, 2010; Streets et al., 2003; Klimont et al., 2011). Comparison of the emissions inventories has revealed large differences in these emissions estimates. Kurokawa et al. (2013) compared different emissions inventories for several provinces in China and found that the difference in primary organic carbon emissions can be as high as 140 %. The possible causes for such discrepancies among emissions inventories are differences in estimates of: (1) activity level, (2) level of technologies implemented, and (3) emission factors. Since it is hard to measure emission factors of each individual source at the scale of a province or a country, uncertainties arise when emission factors from one place are applied to another. Activity data or emission factors are often not available at the level of detail required for making insightful comparisons across emissions inventories.

While comparison of emissions inventories has revealed notable differences in the emissions estimates, few studies have addressed to what extent uncertainty in the emissions inventories really matters for the outcome of air quality modeling studies. Ma and van Aardenne (2004) compared simulated surface O_3 mixing ratios over China using three different emissions inventories as model inputs, and found that surface O_3 differed as much as 30-50 % among different model simulations. They also demonstrated that the differences in NO_x and non-methane volatile organic compounds (NMVOCs) among different inventories were dominant factors for the discrepancies in simulated O_3 mixing ratios. Amnuaylojaroen et al. (2014), on the other hand, studied the effect of different anthropogenic emissions inventories on air quality over Southeast Asia and found only a small difference in simulated O_3 (about 4.5 %) and CO (about 8 %) mixing ratios. However, these studies did not investigate the impact of emissions inventories on other pollutant species such as PM. *Unlike the previous studies, which focused on uncertainties of simulated O_3, CO and NO_x, this study provides quantitative information on how emissions inventories impact PM and other pollutants including SO_2.*

The first objective of this paper is to study the sensitivity of regional air quality to emissions. We select two commonly used anthropogenic emissions inventories for comparison: the Regional Emission Inventory in ASia version 2 (REAS) (Kurokawa et al., 2013) and the Emissions Database for Global Atmospheric Research version 4.2 (EDGAR) (JRC and PBL, 2010). By comparing the 2-week model simulations using these two emissions inventories and observations from July 2007, we select the REAS inventory to perform air quality simulations over East Asia in different seasons. The second objective is to evaluate the simulated PM_{10} concentrations, as well as O_3, SO_2, and NO_x mixing ratios from four one-month WRF-Chem runs against ground-level observations to build confidence in its ability to simulate future air quality over this region. *WRF-Chem is an online-coupled meteorology and chemistry model, simulating meteorological quantities and air pollution concentrations simultaneously and allowing two-way interactions between meteorological and chemical constituents. In regions with high PM loading, meteorology-chemistry interaction significantly improves model performance in simulating air pollutant concentrations (Kong et al., 2015).* So far, many of the WRF-Chem studies that focused on China conducted limited model evaluation due to

the scarcity of observations in the region. This study compares the model simulations to observations from more than 70 sites in China to evaluate the model. There are some studies that have compared simulation results using a different chemical transport model (i.e., the Community Multi-scale Air Quality Model), but as far as we are aware, few studies have used as extensive a network of PM_{10} observations for WRF-Chem validation in this region as ours has.

This paper is organized as follows. Section 2 explains the regional air quality model (WRF-Chem) configuration, emissions used for the model, observations used for validation, and data analysis methods. Section 3 analyzes the differences in emissions inventories and the sensitivity of simulated pollutant concentrations to the inventory used. Section 4 evaluates model performance by comparing observations with model simulations. Section 5 presents a summary of results and suggestions for future research.

2 Model and observations description

2.1 Model description

We use the fully coupled "online" regional chemical transport model WRF-Chem version 3.5 (Grell et al., 2005) in this study. The Regional Acid Deposition Model version 2 (RADM2) atmospheric chemical mechanism (Stockwell et al., 1990) is used for gas-phase chemistry. Aerosol chemistry is represented by the Model Aerosol Dynamics for Europe with the Secondary Organic Aerosol Model (MADE/SORGAM) (Schell et al., 2001; Ackermann et al., 1998) with some aqueous reactions. This aerosol mechanism is widely used in regional atmospheric chemistry models (Saikawa et al., 2011; Gao et al., 2014; Tuccella et al., 2012; Kumar et al., 2012). It predicts the mass of seven aerosol species (sulfate, ammonium, nitrate, sea salt, BC, OC, and secondary organic aerosols), using three log-normal aerosol modes (Aitken, accumulation, and coarse). Aerosol dry deposition is simulated following the approach of Binkowski and Shankar (1995) and the wet removal approach follows Easter et al. (2004) and Chapman et al. (2009). Photolysis rates are obtained from the Fast-J photolysis scheme (Wild et al., 2000). *We include the aerosol-radiative feedback in our simulation. The rapid radiative transfer model (RRTM) scheme (Mlawer et al., 1997) is used to represent both shortwave and longwave radiation. The horizontal winds, temperature, and moisture are nudged to 2007 meteorological fields at all vertical levels. The 2007 meteorological data are obtained from the National Center for Environmental Prediction (NCEP) Global Forecast System final gridded analysis datasets.* We use the Lin et al. (1983) microphysics scheme and the Grell-3d ensemble cumulus parameterization(Grell and Dévényi, 2002).

The model domain, shown in Fig. 1, covers most of the East and South Asia region with 398 × 298 grid cells, using a 20-km spacing and a Lambert conformal map projection centered on China at 32°N, 100°E. There are 31 vertical levels from the surface to 50 mb. The initial and lateral boundary conditions are taken from a time-slice simulation of the GFDL coupled chemistry-climate model

4

AM3 (Donner et al., 2011; Naik et al., 2013) for year 2010 following the configuration described by Naik et al. (2013). This AM3 simulation was driven by climatological mean sea-surface temperature and sea ice distributions for the 2006-2015 time period derived from the transient GFDL coupled model (GFDL-CM3) simulations following the Representative Concentration Pathway 8.5 (RCP8.5) (John et al., 2012). Concentrations of well-mixed greenhouse gases and ozone depleting substances, and emissions of short-lived pollutants (ozone precursors and aerosols) were set to year 2010 values in RCP8.5. We simulate air pollutant concentrations for the central month of each season (January, April, July, and October) in 2007, to assess seasonal variability in air quality. The model is spun-up for seven days before the beginning of each monthly simulation. This is sufficient to ventilate our regional domain.

2.2 Emissions

The anthropogenic emissions of gaseous pollutants (CO, NO_x, NH_3, SO_2, and NMVOCs) and particulate matter (BC, OC, $PM_{2.5}$, and PM_{10}) are taken from REAS (Kurokawa et al., 2013). REAS covers most of the model domain (see Fig. 1, regions in blue). For the areas of our domain that are not covered by the REAS emissions inventory, we use the RCP8.5 emissions dataset for year 2010 (Riahi et al., 2011). RCP8.5 emissions dataset has been used in many studies for air quality simulations (Gao et al., 2013; Colette et al., 2013; Fry et al., 2012). For emissions from biomass burning, we use the year 2007 from the Global Fire Emissions Database version 3 (GFED) (Randerson et al., 2013). For biogenic emissions of CO, NO_x, and NMVOCs, as well as aircraft emissions of CO, NO_x, and SO_2, we use the Precursors of Ozone and their Effect on the Troposphere version 1 (POET) emissions inventory (Granier et al., 2005). Dust and sea salt emissions are calculated online using the dust transport model (Shaw et al., 2008) and sea salt (Gong, 2003) schemes, respectively.

To study the influence of anthropogenic emissions inventories on air quality simulation, we conducted a sensitivity simulation using the EDGAR (European Commission Joint Research Centre, 2010) inventory, as described in Section 3. EDGAR does not provide BC, OC, and $PM_{2.5}$ emissions, and thus, this study only compares simulated O_3 and PM_{10}. NMVOCs in EDGAR are also not speciated, so we divided them into 17 chemical species, using weighting factors calculated from REAS. The total anthropogenic emissions of each air pollutant within the model domain as estimated in REAS and EDGAR for July 2007 are listed in Table 1. *We apply the same diurnal variation to both REAS and EDGAR. REAS emissions inventory provides monthly emissions for each pollutant, while the EDGAR emissions inventory provides only yearly emissions estimates.*

2.3 Observations

The surface concentrations of PM_{10} in China are derived from the Air Pollution Index (API) from the website of the Ministry of Environmental Protection of the People's Republic of China (http://datacenter.mep.gov.cn/). When PM_{10} is reported as the primary pollutant with a maximum pollutant index, daily PM_{10} con-

centrations are calculated from the API, using the following equation:

$$C = [(I - I_{low})/(I_{high} - I_{low})] \times (C_{high} - C_{low}) + C_{low} \qquad (1)$$

where C is the daily concentration of PM_{10}, I is the API reported, I_{low} and I_{high} are the lower and upper API breakpoints that I falls within, C_{low} and C_{high} are the PM_{10} concentrations corresponding to I_{low} and I_{high}. Values of I_{low}, I_{high}, C_{low} and C_{high} are described for different API levels, as shown in Table S1. Qu et al. (2010) have shown that API-derived PM_{10} concentrations are generally comparable to those from filter sampling, although the latter tends to be approximately 10% higher than API-derived PM_{10}. As mentioned earlier, the derived concentrations from API have been used for the evaluation of a different chemical transport model in previous studies (Wang et al., 2009; Liu et al., 2010).

The observed PM_{10} concentrations in Nepal are obtained from the Godavari station, located at the southern edge of the Kathmandu Valley (Ramanathan et al., 2007; Stone et al., 2010). *We are unable to evaluate* $PM_{2.5}$ *against measurements for 2007 since* $PM_{2.5}$ *measurements in China started in late 2012.* The observed PM_{10}, O_3, and SO_2 in Japan and SO_2 and NO_2 in China are taken from the Acid Deposition Monitoring Network in East Asia (EANET). The surface mixing ratios of O_3 in Mt. Lulin are taken from the Lulin Atmospheric Background Station (LABS, 2,862m above mean sea leave) in central Taiwan (Ou Yang et al., 2012). The description of each site is listed in Tables S2a-b; the locations of these sites are shown in Fig. 1.

2.4 Data analysis method

We assess the model performance using the correlation coefficient (r), the normalized mean bias (NMB), the mean fractional bias (MFB), the mean fractional error (MFE), and the normalized mean square error (NMSE) between the observed (Obs) and modeled (Model) concentrations. The performance evaluation is based on monthly and yearly statistics using the daily mean values at each site, each region, and all sites. *Following Boylan and Russell (2006), we set the performance goals of* PM_{10} *as: MFB less than or equal to* ±30 *% and MFE less than or equal to 50 %. The performance criteria of* PM_{10} *are MFB* $\leqslant \pm 60$ *% and MFE* $\leqslant 75$ *%.* For O_3, we use the performance benchmark: MFB $\leqslant \pm15$ % and MFE $\leqslant 35$ %, as recommended by Morris et al. (2005).

3 Sensitivity to emissions

To better understand the effect that anthropogenic emissions have on regional air quality simulations, we conduct two simulations in which REAS and EDGAR are used as separate inputs. In the following sections, we compare the major pollutant emissions estimated in REAS and EDGAR, followed by comparisons of resulting air quality simulations.

3.1 Emission comparisons

Table 1 summarizes the total emissions of major air pollutants over the model domain in July 2007 for air pollutant precursors. Both REAS and EGAR estimate similar total SO_2 emissions of 4.62 Tg month^{-1}. *We note that this similarity is purely coincidental and depends on the domain. In certain parts of the domain REAS estimate is higher than EDGAR, while the opposite is true for other parts of the domain. When averaged over the whole domain, both inventories produce similar estimates (Fig. 2).* We, however, find large discrepancies between REAS and EDGAR estimated emissions for total NH_3 (53 %) and NO_x (27 %). For CO, NH_3, and NO_x, REAS estimates are higher than those of EDGAR, while for PM_{10} and NMVOCs, the opposite is the case. Figure 2 illustrates the difference in the spatial distribution and magnitude of emissions between REAS and EDGAR for PM_{10}, CO, SO_2, and NO_x in our model domain. Although the total emissions within the domain for many of the species are comparable between the two inventories, the national and regional differences are large. REAS estimates are uniformly higher than those of EDGAR in North, East, and South China for all four species and in most parts of India for NO_x and CO. For PM_{10} and CO, EDGAR estimates are higher in most areas of South and Southeast Asia, as well as in Japan and South Korea. Table S3 compares the differences in provincial emissions between REAS and EDGAR in China. For example, we find that REAS estimates 150 % higher PM_{10} and 548 % higher CO emissions than EDGAR in Hebei province.

3.2 Simulation comparisons

For the convenience of discussion, we refer to the simulation with REAS emissions as WRF-Chem-REAS and the simulation using EDGAR emissions as WRF-Chem-EDGAR. Figure 3 illustrates the differences in the 14-day mean PM_{10}, O_3, SO_2, and NO_2 simulated from July 1 to July 14, 2007. The difference is presented as the percentage difference in concentrations or mixing ratios relative to those simulated in WRF-Chem-EDGAR. The pattern of the difference for these species is similar to that of emissions difference. WRF-Chem-REAS simulates 40–70 % higher surface PM_{10} in most areas of the North China Plain (Beijing, Tianjin, Hebei, Henan, Shandong province). This difference, around 35 μg m^{-3} or higher, is comparable to the PM_{10} levels in many sites in Japan (Table 3). The highest difference (70 %) occurs in Shandong province and the lowest difference (less than ±5 %) is found in western China (Table S3). WRF-Chem-EDGAR simulates higher PM_{10} than WRF-Chem-REAS around Cambodia, Vietnam, and Thailand. For surface O_3, a moderate difference of 16–20 % (approximately 12–16 ppbv) is found over the North China Plain, the Yangtze River Delta, Central China, and eastern Pakistan. WRF-Chem-REAS also results in higher SO_2 and NO_2 (more than 10 ppbv) in these areas than WRF-Chem-EDGAR. The largest discrepancies, over 100 %, occur in Guizhou (220 %) and Yunnan (175 %) provinces for SO_2, and in Shanghai (258 %) and Shandong (118 %) provinces for NO_2.

7

Table 2 summarizes the statistical measures of model simulations using these two anthropogenic emissions inventories against observations. Both simulations reproduce the temporal variation of O_3, SO_2, and NO_2 well, with the value of r between 0.64 and 0.83. The temporal correlation of PM_{10} for WRF-Chem-REAS ($r = 0.38$) is higher than that calculated for WRF-Chem-EDGAR ($r = 0.2$). In terms of bias, both simulations produce similar NMB and MFB for O_3. For PM_{10}, NO_2, and SO_2, WRF-Chem-REAS has a smaller MFB than WRF-Chem-EDGAR. In terms of error, MFE and NMSE from the two simulations are comparable for O_3 but WRF-Chem-REAS results in less MFE and NMSE for PM_{10} and NO_2. According to the model performance goals and criteria of PM_{10} suggested by Boylan and Russell (2006), WRF-Chem-EDGAR meets the performance criteria, while WRF-Chem-REAS achieves the stricter performance goals. *We have conducted additional sensitivity simulations using REAS and EDGAR in January and July and compared the simulated air pollutants and observation. The results of these two-month simulations (not shown here) agree with what we find here.*

Based on the above performance analyses, we choose REAS as the anthropogenic emissions inventory to conduct further simulations for four months to explore the seasonality of air pollutant concentrations. In this paper, we focus on validating the WRF-Chem model with REAS.

4 Spatiotemporal variations of pollutants and model evaluation

In this section, we analyze the spatial variability of simulated and observed monthly mean PM_{10} concentrations, as well as O_3, SO_2, and NO_x mixing ratios (Figs. 4, 7, 9, and 10). A color-filled circle overlaid on a model-simulated monthly average surface concentration map represents the observed monthly-average value at each site. Tables 3–6 describe yearly statistics for PM_{10} concentrations, as well as O_3, SO_2, and NO_2 mixing ratios at individual stations, respectively. Table S6 summarizes seasonal statistics for the same pollutants at all available stations. The comparisons between daily modeled and observed concentrations of each pollutant are given in Figs. 5, 6, 8, and 11 for individual sites. Detailed analyses of model biases and errors for each of the species are provided in the following subsections.

Before evaluating the model performance in simulating air pollutants, we evaluate the simulated meteorological fields, including daily mean 2 m temperature, 2 m relative humidity, and 10 m wind speed against observations from National Climate Data Center of China Meteorological Administration for year 2007 (Table S4). The model reproduces 2 m temperature with a correlation of 0.97 and a negative NMB of -14.57 %. Relative humidity is simulated with a correlation of 0.71 and a positive NMB of 7.02 %. Compared to temperature and relative humidity, the 10 m wind speed has a relatively lower correlation of 0.52 and a higher positive NMB of 59.35 %. Overall, the model performance in simulating these meteorological data is similar to that reported for regional air quality models (Tuccella et al., 2012; Tessum et al., 2015; Zhang et al., 2015).

4.1 PM_{10}

265 We obtain ground-level measurements from one site in Nepal, seven sites in Japan, and 71 sites in
China. China is divided into seven geographical regions and measurements are analyzed, based on
these regions (Table 3). The coverage of each geographical region in China is shown in Figure S1.
In China, the highest 4-month average PM_{10} is observed in the Northwest (126 ± 94 μg m^{-3}),
followed by the Northeast (119 ± 65 μg m^{-3}) and Central China (117 ± 48 μg m^{-3}), while the
270 lowest observed PM_{10} is in South China (82 ± 28 μg m^{-3}). In Japan, the observed four-month
average PM_{10} concentration is 27 ± 33 μg m^{-3}, which is more than three times lower than those
observed in China.

The model simulates high PM_{10} concentrations (over 200 μg m^{-3}) near the Gobi Desert in North-
west China and in the border area near Iran, Afghanistan, and Pakistan (Fig. 4). In these areas, dust
275 emissions are the predominant source of PM_{10} and the anthropogenic primary PM_{10} is negligible as
shown in Fig. S2. Besides these areas, the model simulates high PM_{10} concentrations (up to 100 μg
m^{-3}) over the North China Plain, the Yangtze River Delta region, and the Sichuan Basin. The model
simulates relatively low PM_{10} concentrations (lower than 60 μg m^{-3}) in most of South, Southwest,
and Northeast China, most of India, and other countries in the model domain. Unlike Northwest
280 China, where the maximum PM_{10} concentrations are simulated in spring, other regions of China
are simulated to have high concentrations in January and October with low concentrations in April
and July. This is because in winter, reduced precipitation leads to higher PM_{10} concentrations, while
the monsoon circulation brings in clean marine air and dilutes the PM_{10} surface concentrations in
eastern China in summer. Moreover, aerosols in summer are removed by wet scavenging due to
285 more frequent precipitation (Zhao et al., 2010). High concentrations are also simulated in an area
surrounding Lhasa in Tibet in January. Since primary anthropogenic emissions in Tibet are low,
dust emissions from local soils on the Plateau are the main reason for high PM_{10} concentrations.
The previous study of tracer element analyses has shown that local dust is the major source of total
particulate matter (PM) over Tibet (Zhang et al., 2001).

290 For 4-month averaged PM_{10}, the model meets the performance criteria at 84 % of observation
sites in China. The model tends to underestimate observations at the rest of the sites, which are
mainly located in Northeast and Southwest China. Analyzing model-observation comparison by re-
gion, we find better model performance at Central, East, North, and South China (Table 3). However,
Northeast and Southwest China have a higher correlation ($r > 0.35$) than others. For sites outside of
295 China, the model underestimates observations in both Japan (MFB = –32 %) and Nepal (MFB = –48
%).

The seasonal statistics (Table S5) and Figures 5-6 indicate that the model meets the performance
criteria in all fourth months (January, April, July, and October) in Central, East, North and South
China. In the remaining regions in China and Japan, model meets or is close to the criteria in April,
300 July and October, but has more difficulty reproducing PM_{10} concentrations in January. Previous

9

research has suggested that poor model performance in winter is common among air quality models and may be caused by difficulty in simulating stagnant weather conditions that lead to high winter PM concentrations (Tessum et al., 2015). In Nepal, model performance in both January and April is poor when the observed PM_{10} is high. The time series comparison plots (Fig. S3) reveal distinct air

305 pollution episodes occurring in middle January and early April at the Godavari site, which the model fails to simulate. One of the possible reasons for this is that the model is unable to reproduce the local meteorology due to the complicated topography that is not well-resolved at the current horizontal resolution. The temporal correlations of all sites in each month are similar (0.37–0.39) as shown in Table S6 and we do not observe obvious trends of temporal correlations change with seasons.

310 ## 4.2 O_3

Similar to PM_{10}, the simulated O_3 over the model domain also exhibits a seasonal variability that varies by region. Figure 7 illustrates that the highest O_3 mixing ratio (over 70 ppbv) occurs in North and East China in July. This is because biogenic NMVOC emissions are relatively high and active photochemical reactions constitute favorable conditions for the build-up of O_3 mixing ratios

315 in summer. On the other hand, a low monthly mean mixing ratio (below 40 ppbv) is found in the same region in January. In the Tibetan Plateau, the surface O_3 mixing ratio reaches a maximum (over 70 ppbv) in April due to high elevations and downward transport of O_3 from the stratosphere, while the minimum O_3 (40 ppbv) is found in July because the upward transport of air to the stratosphere in the summer suppresses the downward transport of O_3 (Gettelman et al., 2004; Randel et al., 2010).

320 This simulated seasonal variability of O_3 in our model over the Tibetan Plateau is consistent with the findings of Ma et al. (2014).

The model performs well for simulating O_3 at all sites in Japan, and both MFB and MFE of these sites are within or close to the model benchmark (MFB < ± 15 % and MFE < 35 %). The model overestimates O_3 at Lulin in Taiwan. MFB at Lulin (41 %) is more than two times higher than that of

325 any sites in Japan. *Statistical analysis of O_3 in different seasons at the Lulin site (Table S7) reveals that such high bias is mainly caused by overestimation in October (MFB = 63 %). A previous study by Ou Yang et al. (2012) suggested that Lulin has more pronounced mountain valley circulation in fall, which leads to low observed O_3 mixing ratios in October. Our model with a horizontal resolution of 20 km × 20 km may not be able to capture such local meteorology.* The model reproduces the

330 overall daily temporal variation of O_3 well (r = 0.57) and the value of temporal correlation is also high for each site (0.47–0.93) except at Rishiri. This is partly due to the lateral boundary conditions, since this site is located close to the northeast boundary of the model domain. The model predicts the seasonal variability well, as shown in Fig. 8 and Table S6. The modeled and observed monthly mean O_3 has a maximum in April and a minimum in July. The same seasonal characteristics of

335 O_3 level were reported before (Yamaji et al., 2006). The MFB and MFE of all sites in each month

are in the acceptable range. Among the four months, the model tends to underestimate the highest observations in April, while it overestimates observations in the other three months.

4.3 SO$_2$ and NO$_2$

Figure 9 illustrates that the model simulates high monthly mean SO$_2$ mixing ratio (higher than 20 ppbv) over urban areas in North China (including Beijing, Tianjin, Hebei, and Shanxi), and some provinces in East China (including Shandong and Henan), where emissions are also the highest. In these areas, the mixing ratios are the highest in January, followed by October, April, and July (Fig. 9). The lowest mixing ratios in our model simulation are found in July due to more active oxidation of SO$_2$ by hydroxyl radical (OH) and O$_3$ in the gas phase, as well as frequent precipitation that favors aqueous-phase oxidation of SO$_2$ (Feichter et al., 1996). Overall, the model predicts SO$_2$ well with MFB of 9 % and r of 0.64. The model performs better in predicting observed SO$_2$ mixing ratios at sites in Japan (MFB = -12–29 %, r = 0.52–0.82) than in China (MFB = -70–63 %, r = 0.14–0.5). The lowest overall MFB value of all sites occurs in April (8 %), while the highest happens in July (31 %). Although MFB values are acceptable, both MFE and NMSE in July and October are high. The site that contributes most to high errors is Beijing, with MFE of more than 115 % in these two months. The model largely overestimates SO$_2$ in Beijing (Fig. 11) probably because the REAS emissions inventory did not take into account the local emissions control policies for the Beijing Olympics. In 2007, the Chinese government reduced anthropogenic emissions by shutting down many polluting industries, banning high-emission vehicles, and restricting the number of on-road vehicles in Beijing (Zhang et al., 2012). It is likely that our emissions were overestimated in Beijing, which caused a large discrepancy between modeled and observed SO$_2$ mixing ratios.

The spatial and seasonal distribution of NO$_2$ is similar to SO$_2$ as shown in Fig. 10. High NO$_2$ mixing ratio is found over Northeast, North, and East China due to high emissions from power plant, industry and transportation sectors in these regions. Outside China, several hot spots are identified, such as Seoul (South Korea) and New Delhi (India). The modeled NO$_2$ mixing ratios have a summer minimum and a winter maximum. The lifetime of NO$_2$ in winter is relatively longer (18–24 hours) than that in summer (6 hours) because the concentration of hydroxyl radical (OH) in atmosphere is low (Beirle et al., 2003). Consequently, the removal reaction of NO$_2$ with OH radical to form HNO$_3$ is less active in winter than in summer. Among the four sites in China, the model performs well in predicting observed NO$_2$ mixing ratios at the Shanghai site (MFB = -9 %); however, it underestimates at the other three sites (MFB > -53 %). WRF-Chem captures the seasonal variability of NO$_2$, but underestimates the monthly average of NO$_2$ with MFB between -41 % and -68 % for all four months. Underestimation of NO$_2$ has also been reported in the South Asian region using WRF-Chem (Kumar et al., 2012) and a possible reason was proposed as the underestimation of NO$_x$ emissions from biomass burning or anthropogenic sources. Another possible reason is that the

11

removal of NO_x was overestimated through the heterogeneous reaction of N_2O_5 to form nitric acid in the WRF-Chem chemical mechanism RADM2 (Yegorova et al., 2011), used in this study.

5 Conclusions

We performed WRF-Chem simulation of air quality over East and South Asia using two different anthropogenic emissions inventories and evaluated the model performance for PM_{10} concentrations, as well as O_3, SO_2, and NO_2 mixing ratios, using ground-level observations for the year 2007. We find that large discrepancies exist between the extensively-used EDGAR global anthropogenic emissions and the REAS regional inventory at national and provincial scales. The discrepancies between these inventories can lead to large differences in simulated surface PM_{10} concentrations (40–70 %), and moderate differences in O_3 mixing ratios (16–20 %) in most areas of North China Plain, as well as more than 100 % differences in SO_2 and NO_2 mixing ratios, found in several provinces in China. Our study demonstrates that WRF-Chem is sensitive to emissions inventories and improvements in emissions inventories are important for accurately simulating regional air quality. Further studies are needed to assess model performance differences due to different emission inputs.

On the basis of lower bias and error values versus observations we found for our WRF-Chem-REAS simulations, we chose the REAS inventory to conduct four one-month simulations for the purpose of model evaluation. The model results indicate clear regional variations in the seasonal cycle of surface PM_{10} and O_3 over East and South Asia. In Northwest China, maximum PM_{10} occurs in April, while in Nepal and other regions of China, the highest PM_{10} mainly occurs in January. For surface O_3 mixing ratios, the peak values are simulated in July for North and East China, and in April for Tibet and Japan. Comparisons between model simulations and observations show that the model performs well in simulating surface PM_{10} and O_3, meeting air quality model performance criteria for both PM_{10} and O_3 at most sites, although the model underestimates PM_{10} at some sites in China in January. The model predicts SO_2 better at sites in Japan than in China, where overestimation is large at the Beijing site in July and October. The model underestimates most observed NO_2 in all four months.

Quantifying uncertainties of simulated air quality at the provincial level due to emission inputs reveals that the uncertainty in emissions inventories leads to significant differences in simulated levels of air pollutants, especially PM_{10}, SO_2 and NO_2. For O_3, on the contrary, different emissions inventories lead to only a moderate variability, showing agreement with the findings of previous studies (Ma and van Aardenne, 2004; Amnuaylojaroen et al., 2014). Our study highlights the importance of better constraining emissions at the provincial level for regional air quality modeling over East Asia, where anthropogenic emissions are high and air pollution is a major environmental and public health challenge. Model evaluation results also indicate that emissions inventories that do not consider local emissions control policies could cause large discrepancies. Our results suggest that

12

future work should focus on better constraining the provincial-level emissions especially estimating the primary PM, SO_2 *and* NO_x.

Code availability

The WRF-Chem model is an open-source, publicly available, and continually improved soft-
410 ware. The version 3.5 used in this study can be downloaded at http://www2.mmm.ucar.edu/wrf/users/download/get_source.html. Known problems of the WRF-Chem version 3.5 have been fixed, using solutions provided online at http://ruc.noaa.gov/wrf/WG11/known-prob_v3.5.htm. We have optimized dust parameterizations in the code, using observed ground-level PM_{10} concentrations. The modified code can be obtained from the corresponding authors.

References

Ackermann, I. J., Hass, H., Memmesheimer, M., Ebel, A., Binkowski, F. S., and Shankar, U.: Modal aerosol dynamics model for Europe: development and first applications, Atmospheric Environment, 32, 2981–2999, doi:http://dx.doi.org/10.1016/S1352-2310(98)00006-5, http://www.sciencedirect.com/science/article/pii/S1352231098000065, 1998.

Amnuaylojaroen, T., Barth, M. C., Emmons, L. K., Carmichael, G. R., Kreasuwun, J., Prasitwattanaseree, S., and Chantara, S.: Effect of different emission inventories on modeled ozone and carbon monoxide in Southeast Asia, Atmospheric Chemistry and Physics, 14, 12 983–13 012, doi:10.5194/acp-14-12983-2014, http://www.atmos-chem-phys.net/14/12983/2014/, 2014.

Beirle, S., Platt, U., Wenig, M., and Wagner, T.: Weekly cycle of NO_2 by GOME measurements: a signature of anthropogenic sources, Atmos. Chem. Phys., 3, 2225–2232, doi:10.5194/acp-3-2225-2003, http://www.atmos-chem-phys.net/3/2225/2003/, 2003.

Binkowski, F. S. and Shankar, U.: The Regional Particulate Matter Model: 1. Model description and preliminary results, Journal of Geophysical Research: Atmospheres, 100, 26 191–26 209, doi:10.1029/95JD02093, http://dx.doi.org/10.1029/95JD02093, 1995.

Boylan, J. W. and Russell, A. G.: PM and light extinction model performance metrics, goals, and criteria for three-dimensional air quality models, Atmospheric Environment, 40, 4946–4959, doi:http://dx.doi.org/10.1016/j.atmosenv.2005.09.087, http://www.sciencedirect.com/science/article/pii/S1352231006000690, 2006.

Chapman, E. G., Gustafson Jr, W. I., Easter, R. C., Barnard, J. C., Ghan, S. J., Pekour, M. S., and Fast, J. D.: Coupling aerosol-cloud-radiative processes in the WRF-Chem model: Investigating the radiative impact of elevated point sources, Atmos. Chem. Phys., 9, 945–964, doi:10.5194/acp-9-945-2009, http://www.atmos-chem-phys.net/9/945/2009/, 2009.

Chen, Z., Wang, J.-N., Ma, G.-X., and Zhang, Y.-S.: China tackles the health effects of air pollution, The Lancet, 382, 1959–1960, http://linkinghub.elsevier.com/retrieve/pii/S0140673613620644, 2013.

Colette, A., Bessagnet, B., Vautard, R., Szopa, S., Rao, S., Schucht, S., Klimont, Z., Menut, L., Clain, G., Meleux, F., Curci, G., and Rouïl, L.: European atmosphere in 2050, a regional air quality and climate perspective under CMIP5 scenarios, Atmos. Chem. Phys., 13, 7451–7471, doi:10.5194/acp-13-7451-2013, http://www.atmos-chem-phys.net/13/7451/2013/, 2013.

Donner, L. J., Wyman, B. L., Hemler, R. S., Horowitz, L. W., Ming, Y., Zhao, M., Golaz, J.-C., Ginoux, P., Lin, S. J., Schwarzkopf, M. D., Austin, J., Alaka, G., Cooke, W. F., Delworth, T. L., Freidenreich, S. M., Gordon, C. T., Griffies, S. M., Held, I. M., Hurlin, W. J., Klein, S. A., Knutson, T. R., Langenhorst, A. R., Lee, H.-C., Lin, Y., Magi, B. I., Malyshev, S. L., Milly, P. C. D., Naik, V., Nath, M. J., Pincus, R., Ploshay, J. J., Ramaswamy, V., Seman, C. J., Shevliakova, E., Sirutis, J. J., Stern, W. F., Stouffer, R. J., Wilson, R. J., Winton, M., Wittenberg, A. T., and Zeng, F.: The Dynamical Core, Physical Parameterizations, and Basic Simulation Characteristics of the Atmospheric Component AM3 of the GFDL Global Coupled Model CM3, Journal of Climate, 24, 3484–3519, doi:10.1175/2011JCLI3955.1, http://dx.doi.org/10.1175/2011JCLI3955.1, 2011.

Easter, R. C., Ghan, S. J., Zhang, Y., Saylor, R. D., Chapman, E. G., Laulainen, N. S., Abdul-Razzak, H., Leung, L. R., Bian, X., and Zaveri, R. A.: MIRAGE: Model description and evaluation of aerosols and trace gases,

14

465 Journal of Geophysical Research: Atmospheres, 109, doi:10.1029/2004JD004571, http://dx.doi.org/10.1029/2004JD004571, 2004.

Feichter, J., Kjellström, E., Rodhe, H., Dentener, F., Lelieveldi, J., and Roelofs, G.-J.: Simulation of the tropospheric sulfur cycle in a global climate model, Atmospheric Environment, 30, 1693–1707, doi:http://dx.doi.org/10.1016/1352-2310(95)00394-0, http://www.sciencedirect.com/science/article/
470 pii/1352231095003940, 1996.

Fry, M. M., Naik, V., West, J. J., Schwarzkopf, M. D., Fiore, A. M., Collins, W. J., Dentener, F. J., Shindell, D. T., Atherton, C., Bergmann, D., Duncan, B. N., Hess, P., MacKenzie, I. A., Marmer, E., Schultz, M. G., Szopa, S., Wild, O., and Zeng, G.: The influence of ozone precursor emissions from four world regions on tropospheric composition and radiative climate forcing, Journal of Geophysical Research: Atmospheres, 117,
475 D07 306, doi:10.1029/2011JD017134, http://dx.doi.org/10.1029/2011JD017134, 2012.

Gao, Y., Fu, J. S., Drake, J. B., Lamarque, J. F., and Liu, Y.: The impact of emission and climate change on ozone in the United States under representative concentration pathways (RCPs), Atmos. Chem. Phys., 13, 9607–9621, doi:10.5194/acp-13-9607-2013, http://www.atmos-chem-phys.net/13/9607/2013/, 2013.

Gao, Y., Zhao, C., Liu, X., Zhang, M., and Leung, L. R.: WRF-Chem simulations of aerosols
480 and anthropogenic aerosol radiative forcing in East Asia, Atmospheric Environment, 92, 250–266, doi:http://dx.doi.org/10.1016/j.atmosenv.2014.04.038, http://www.sciencedirect.com/science/article/pii/S1352231014003100, 2014.

Gettelman, A., Kinnison, D. E., Dunkerton, T. J., and Brasseur, G. P.: Impact of monsoon circulations on the upper troposphere and lower stratosphere, Journal of Geophysical Research: Atmospheres, 109, D22 101,
485 doi:10.1029/2004JD004878, http://dx.doi.org/10.1029/2004JD004878, 2004.

Gong, S. L.: A parameterization of sea-salt aerosol source function for sub- and super-micron particles, Global Biogeochemical Cycles, 17, 1097, doi:10.1029/2003GB002079, http://dx.doi.org/10.1029/2003GB002079, 2003.

Granier, C.Lamarque, J. F., Mieville, A., Muller, J. F., Olivier, J., Orlando, J., Peters, J., Petron, G., Tyn-
490 dall, G., and Wallens, S.: POET, a database of surface emissions of ozone precursors, available at: http://www.aero.jussieu.fr/projet/ACCENT/POET.php,, 2005.

Grell, G. A. and Dévényi, D.: A generalized approach to parameterizing convection combining ensemble and data assimilation techniques, Geophysical Research Letters, 29, 38–1–38–4, doi:10.1029/2002GL015311, http://dx.doi.org/10.1029/2002GL015311, 2002.

495 Grell, G. A., Peckham, S. E., Schmitz, R., McKeen, S. A., Frost, G., Skamarock, W. C., and Eder, B.: Fully coupled "online" chemistry within the WRF model, Atmospheric Environment, 39, 6957–6975, doi:http://dx.doi.org/10.1016/j.atmosenv.2005.04.027, http://www.sciencedirect.com/science/article/pii/S1352231005003560, 2005.

HEI: Outdoor air pollution among top global health risks in 2010., http://www.healtheffects.org/International/
500 HEI-India-GBD-PressRelease021313.pdf, 2013.

John, J. G., Fiore, A. M., Naik, V., Horowitz, L. W., and Dunne, J. P.: Climate versus emission drivers of methane lifetime against loss by tropospheric OH from 1860–2100, Atmos. Chem. Phys., 12, 12 021–12 036, doi:10.5194/acp-12-12021-2012, http://www.atmos-chem-phys.net/12/12021/2012/, 2012.

JRC and PBL: Emission Database for Global Atmospheric Research (EDGAR), version 4.2., European Commission, Joint Research Centre/PBL Netherlands Environmental Assessment Agency, http://edgar.jrc.ec.europa.eu, 2010.

505

Klimont, Z., Cofala, J., Xing, J., Wei, W., Zhang, C., Wang, S., Kejun, J., Bhandari, P., Mathur, R., Purohit, P., Rafaj, P., Chambers, A., Amann, M., and Hao, J.: Projections of SO 2 , NO x and carbonaceous aerosols emissions in Asia, Tellus B, 61, http://www.tellusb.net/index.php/tellusb/article/view/16858, 2011.

510 Kong, X., Forkel, R., Sokhi, R. S., Suppan, P., Baklanov, A., Gauss, M., Brunner, D., Barò, R., Balzarini, A., Chemel, C., Curci, G., Jiménez-Guerrero, P., Hirtl, M., Honzak, L., Im, U., Pérez, J. L., Pirovano, G., Jose, R. S., Schlünzen, K. H., Tsegas, G., Tuccella, P., Werhahn, J., Žabkar, R., and Galmarini, S.: Analysis of meteorology–chemistry interactions during air pollution episodes using online coupled models within {AQMEII} phase-2, Atmospheric Environment, 115, 527

515 – 540, doi:http://dx.doi.org/10.1016/j.atmosenv.2014.09.020, http://www.sciencedirect.com/science/article/pii/S1352231014007134, 2015.

Kumar, R., Naja, M., Pfister, G. G., Barth, M. C., Wiedinmyer, C., and Brasseur, G. P.: Simulations over South Asia using the Weather Research and Forecasting model with Chemistry (WRF-Chem): chemistry evaluation and initial results, Geosci. Model Dev., 5, 619–648, doi:10.5194/gmd-5-619-2012, http://www.geosci-model-dev.net/5/619/2012/, 2012.

520

Kurokawa, J., Ohara, T., Morikawa, T., Hanayama, S., Janssens-Maenhout, G., Fukui, T., Kawashima, K., and Akimoto, H.: Emissions of air pollutants and greenhouse gases over Asian regions during 2000–2008: Regional Emission inventory in ASia (REAS) version 2, Atmos. Chem. Phys., 13, 11 019– 11 058, doi:10.5194/acp-13-11019-2013, http://www.atmos-chem-phys.net/13/11019/2013/, 2013.

525 Lin, Y.-L., Farley, R. D., and Orville, H. D.: Bulk Parameterization of the Snow Field in a Cloud Model, Journal of Climate and Applied Meteorology, 22, 1065–1092, doi:10.1175/1520-0450(1983)022<1065:BPOTSF>2.0.CO;2, http://dx.doi.org/10.1175/1520-0450(1983)022<1065:BPOTSF>2.0.CO, 1983.

Liu, X.-H., Zhang, Y., Cheng, S.-H., Xing, J., Zhang, Q., Streets, D. G., Jang, C., Wang, W.-X., and Hao, J.-M.:

530 Understanding of regional air pollution over China using CMAQ, part I performance evaluation and seasonal variation, Atmospheric Environment, 44, 2415–2426, doi:http://dx.doi.org/10.1016/j.atmosenv.2010.03.035, http://www.sciencedirect.com/science/article/pii/S135223101000261X, 2010.

Ma, J. and van Aardenne, J. A.: Impact of different emission inventories on simulated tropospheric ozone over China: a regional chemical transport model evaluation, Atmos. Chem. Phys., 4, 877–887, doi:10.5194/acp-

535 4-877-2004, http://www.atmos-chem-phys.net/4/877/2004/, 2004.

Ma, J., Lin, W. L., Zheng, X. D., Xu, X. B., Li, Z., and Yang, L. L.: Influence of air mass downward transport on the variability of surface ozone at Xianggelila Regional Atmosphere Background Station, southwest China, Atmos. Chem. Phys., 14, 5311–5325, doi:10.5194/acp-14-5311-2014, http://www.atmos-chem-phys.net/14/5311/2014/, 2014.

540 Mlawer, E. J., Taubman, S. J., Brown, P. D., Iacono, M. J., and Clough, S. A.: Radiative transfer for inhomogeneous atmospheres: RRTM, a validated correlated-k model for the longwave, Journal of Geophysical Research: Atmospheres, 102, 16 663–16 682, doi:10.1029/97JD00237, http://dx.doi.org/10.1029/97JD00237, 1997.

Morris, R., Koo, B., McNally, D., Tesche, T., and Tonnesen, G.: Application of Multiple Models to Simulation Fine Particulate in the Southeastern US Presented at the National Regional Planning Organizations Modeling Meeting, Denver, CO, 2005.

Naik, V., Horowitz, L. W., Fiore, A. M., Ginoux, P., Mao, J., Aghedo, A. M., and Levy, H.: Impact of preindustrial to present-day changes in short-lived pollutant emissions on atmospheric composition and climate forcing, Journal of Geophysical Research: Atmospheres, 118, 8086–8110, doi:10.1002/jgrd.50608, http://dx.doi.org/10.1002/jgrd.50608, 2013.

Ohara, T., Akimoto, H., Kurokawa, J., Horii, N., Yamaji, K., Yan, X., and Hayasaka, T.: An Asian emission inventory of anthropogenic emission sources for the period 1980-2020, Atmospheric Chemistry and Physics, 7, 4419–4444, doi:10.5194/acp-7-4419-2007, http://www.atmos-chem-phys.net/7/4419/2007/, 2007.

Ou Yang, C.-F., Lin, N.-H., Sheu, G.-R., Lee, C.-T., and Wang, J.-L.: Seasonal and diurnal variations of ozone at a high-altitude mountain baseline station in East Asia, Atmospheric Environment, 46, 279–288, doi:http://dx.doi.org/10.1016/j.atmosenv.2011.09.060, http://www.sciencedirect.com/science/article/pii/S1352231011010235, 2012.

Qu, W. J., Arimoto, R., Zhang, X. Y., Zhao, C. H., Wang, Y. Q., Sheng, L. F., and Fu, G.: Spatial distribution and interannual variation of surface PM_{10} concentrations over eighty-six Chinese cities, Atmos. Chem. Phys., 10, 5641–5662, doi:10.5194/acp-10-5641-2010, http://www.atmos-chem-phys.net/10/5641/2010/, 2010.

Ramanathan, V., Li, F., Ramana, M. V., Praveen, P. S., Kim, D., Corrigan, C. E., Nguyen, H., Stone, E. A., Schauer, J. J., Carmichael, G. R., Adhikary, B., and Yoon, S. C.: Atmospheric brown clouds: Hemispherical and regional variations in long-range transport, absorption, and radiative forcing, Journal of Geophysical Research: Atmospheres, 112, doi:10.1029/2006JD008124, http://dx.doi.org/10.1029/2006JD008124, 2007.

Randel, W. J., Park, M., Emmons, L., Kinnison, D., Bernath, P., Walker, K. A., Boone, C., and Pumphrey, H.: Asian Monsoon Transport of Pollution to the Stratosphere, Science, 328, 611–613, doi:10.1126/science.1182274, http://www.sciencemag.org/content/328/5978/611.abstract, 2010.

Randerson, J., van der Werf, G., Giglio, L., Collatz, G., and Kasibhatla, P.: Global Fire Emissions Database, Version 3 (GFEDv3.1), doi:doi:10.3334/ORNLDAAC/1191, 2013.

Riahi, K., Rao, S., Krey, V., Cho, C., Chirkov, V., Fischer, G., Kindermann, G., Nakicenovic, N., and Rafaj, P.: RCP 8.5—A scenario of comparatively high greenhouse gas emissions, Climatic Change, 109, 33–57, doi:10.1007/s10584-011-0149-y, http://dx.doi.org/10.1007/s10584-011-0149-y, 2011.

Saikawa, E., Kurokawa, J., Takigawa, M., Borken-Kleefeld, J., Mauzerall, D. L., Horowitz, L. W., and Ohara, T.: The impact of China's vehicle emissions on regional air quality in 2000 and 2020: a scenario analysis, Atmos. Chem. Phys., 11, 9465–9484, doi:10.5194/acp-11-9465-2011, http://www.atmos-chem-phys.net/11/9465/2011/, 2011.

Schell, B., Ackermann, I. J., Hass, H., Binkowski, F. S., and Ebel, A.: Modeling the formation of secondary organic aerosol within a comprehensive air quality model system, Journal of Geophysical Research-Atmospheres, 106, 28 275–28 293, <GotoISI>://000172355800019, 2001.

Seinfeld, J. H. and Pandis, S. N.: Atmospheric chemistry and physics: from air pollution to climate change, John Wiley and Sons, 2012.

Shaw, W. J., Jerry Allwine, K., Fritz, B. G., Rutz, F. C., Rishel, J. P., and Chapman, E. G.: An evaluation of the wind erosion module in DUSTRAN, Atmospheric Environment, 42, 1907–

545

550

555

560

565

570

575

580

1921, doi:http://dx.doi.org/10.1016/j.atmosenv.2007.11.022, http://www.sciencedirect.com/science/article/
585   pii/S1352231007010564, 2008.

Stockwell, W. R., Middleton, P., Chang, J. S., and Tang, X.: The second generation regional acid deposition
       model chemical mechanism for regional air quality modeling, Journal of Geophysical Research: Atmo-
       spheres, 95, 16 343–16 367, doi:10.1029/JD095iD10p16343, http://dx.doi.org/10.1029/JD095iD10p16343,
       1990.

590   Stone, E. A., Schauer, J. J., Pradhan, B. B., Dangol, P. M., Habib, G., Venkataraman, C., and Ramanathan,
       V.: Characterization of emissions from South Asian biofuels and application to source apportionment of
       carbonaceous aerosol in the Himalayas, Journal of Geophysical Research: Atmospheres, 115, D06 301,
       doi:10.1029/2009JD011881, http://dx.doi.org/10.1029/2009JD011881, 2010.

Streets, D. G., Bond, T. C., Carmichael, G. R., Fernandes, S. D., Fu, Q., He, D., Klimont, Z., Nelson,
595   S. M., Tsai, N. Y., Wang, M. Q., Woo, J.-H., and Yarber, K. F.: An inventory of gaseous and primary
       aerosol emissions in Asia in the year 2000, Journal of Geophysical Research: Atmospheres, 108, n/a–n/a,
       doi:10.1029/2002JD003093, http://dx.doi.org/10.1029/2002JD003093, 8809, 2003.

Tessum, C. W., Hill, J. D., and Marshall, J. D.: Twelve-month, 12 km resolution North American WRF-Chem
       v3.4 air quality simulation: performance evaluation, Geosci. Model Dev., 8, 957–973, doi:10.5194/gmd-8-
600   957-2015, http://www.geosci-model-dev.net/8/957/2015/, 2015.

Tuccella, P., Curci, G., Visconti, G., Bessagnet, B., Menut, L., and Park, R. J.: Modeling of gas and aerosol with
       WRF/Chem over Europe: Evaluation and sensitivity study, Journal of Geophysical Research: Atmospheres,
       117, D03 303, doi:10.1029/2011JD016302, http://dx.doi.org/10.1029/2011JD016302, 2012.

Wang, K., Zhang, Y., Jang, C., Phillips, S., and Wang, B.: Modeling intercontinental air pollution transport over
605   the trans-Pacific region in 2001 using the Community Multiscale Air Quality modeling system, Journal of
       Geophysical Research: Atmospheres, 114, D04 307, doi:10.1029/2008JD010807, http://dx.doi.org/10.1029/
       2008JD010807, 2009.

Wang, X., Liang, X.-Z., Jiang, W., Tao, Z., Wang, J. X. L., Liu, H., Han, Z., Liu, S., Zhang,
       Y., Grell, G. A., and Peckham, S. E.: WRF-Chem simulation of East Asian air quality: Sen-
610   sitivity to temporal and vertical emissions distributions, Atmospheric Environment, 44, 660–
       669, doi:http://dx.doi.org/10.1016/j.atmosenv.2009.11.011, http://www.sciencedirect.com/science/article/
       pii/S1352231009009558, 2010.

WHO: Ambient Air Pollution Database, http://www.who.int/entity/quantifying_ehimpacts/national/
       countryprofile/AAP_PM_database_May2014.xls?ua=1, 2014.

615   Wild, O., Zhu, X., and Prather, M.: Fast-J: Accurate Simulation of In- and Below-Cloud Photolysis in Tropo-
       spheric Chemical Models, Journal of Atmospheric Chemistry, 37, 245–282, doi:10.1023/A:1006415919030,
       http://dx.doi.org/10.1023/A%3A1006415919030, 2000.

Yamaji, K., Ohara, T., Uno, I., Tanimoto, H., Kurokawa, J.-i., and Akimoto, H.: Analysis of the sea-
       sonal variation of ozone in the boundary layer in East Asia using the Community Multi-scale Air
620   Quality model: What controls surface ozone levels over Japan?, Atmospheric Environment, 40, 1856–
       1868, doi:http://dx.doi.org/10.1016/j.atmosenv.2005.10.067, http://www.sciencedirect.com/science/article/
       pii/S1352231005010794, 2006.

18

Yegorova, E. A., Allen, D. J., Loughner, C. P., Pickering, K. E., and Dickerson, R. R.: Characterization of an eastern U.S. severe air pollution episode using WRF/Chem, Journal of Geophysical Research: Atmospheres, 116, doi:10.1029/2010JD015054, http://dx.doi.org/10.1029/2010JD015054, 2011.

625

Zhang, B., Wang, Y., and Hao, J.: Simulating aerosol–radiation–cloud feedbacks on meteorology and air quality over eastern China under severe haze conditionsin winter, Atmospheric Chemistry and Physics, 15, 2387–2404, doi:10.5194/acp-15-2387-2015, http://www.atmos-chem-phys.net/15/2387/2015/, 2015.

Zhang, X., van Geffen, J., Liao, H., Zhang, P., and Lou, S.: Spatiotemporal variations of tropo-

630

spheric SO_2 over China by SCIAMACHY observations during 2004–2009, Atmospheric Environment, 60, 238–246, doi:http://dx.doi.org/10.1016/j.atmosenv.2012.06.009, http://www.sciencedirect.com/science/article/pii/S1352231012005390, 2012.

Zhang, X. Y., Arimoto, R., Cao, J. J., An, Z. S., and Wang, D.: Atmospheric dust aerosol over the Tibetan Plateau, Journal of Geophysical Research: Atmospheres, 106, 18 471–18 476, doi:10.1029/2000JD900672,

635

http://dx.doi.org/10.1029/2000JD900672, 2001.

Zhao, C., Wang, Y., Yang, Q., Fu, R., Cunnold, D., and Choi, Y.: Impact of East Asian summer monsoon on the air quality over China: View from space, Journal of Geophysical Research: Atmospheres, 115, D09 301, doi:10.1029/2009JD012745, http://dx.doi.org/10.1029/2009JD012745, 2010.
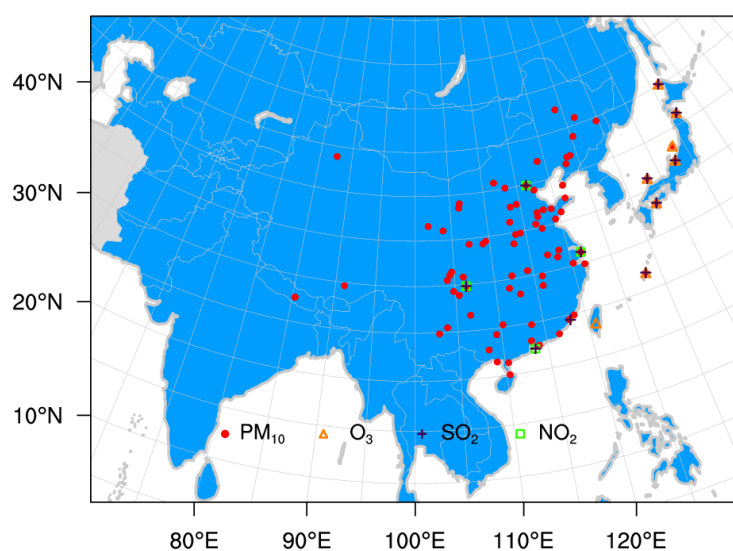
19

Figure 1. WRF-Chem model domain and observation sites. Blue shading indicates locations where the REAS emissions inventory is used. Gray shading indicates where the RCP8.5 emissions are used. For the entire model domain, biomass burning emissions from GFED v3 and biogenic emissions from POET v1 are used. Red-filled circles denote the observational sites with PM_{10}; orange triangles for sites with O_3; purple crosses for sites with SO_2; and green squares for sites with NO_2.
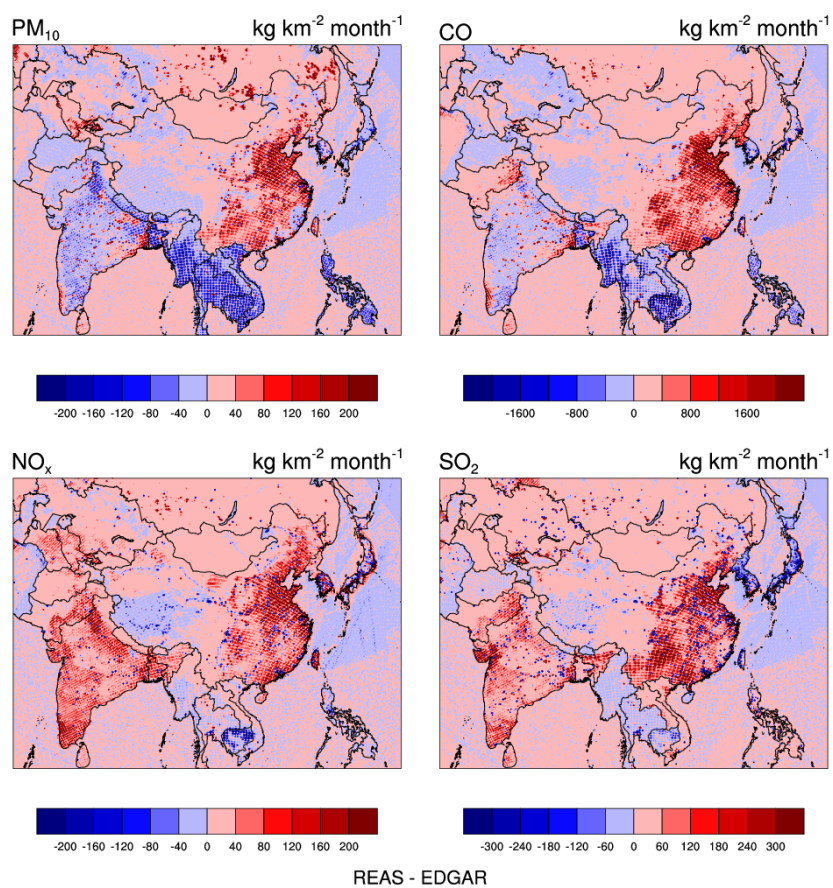
Figure 2. Monthly emissions difference of PM_{10}, CO, SO_2, and NO_x between REAS and EDGAR in July 2007 in our model domain.
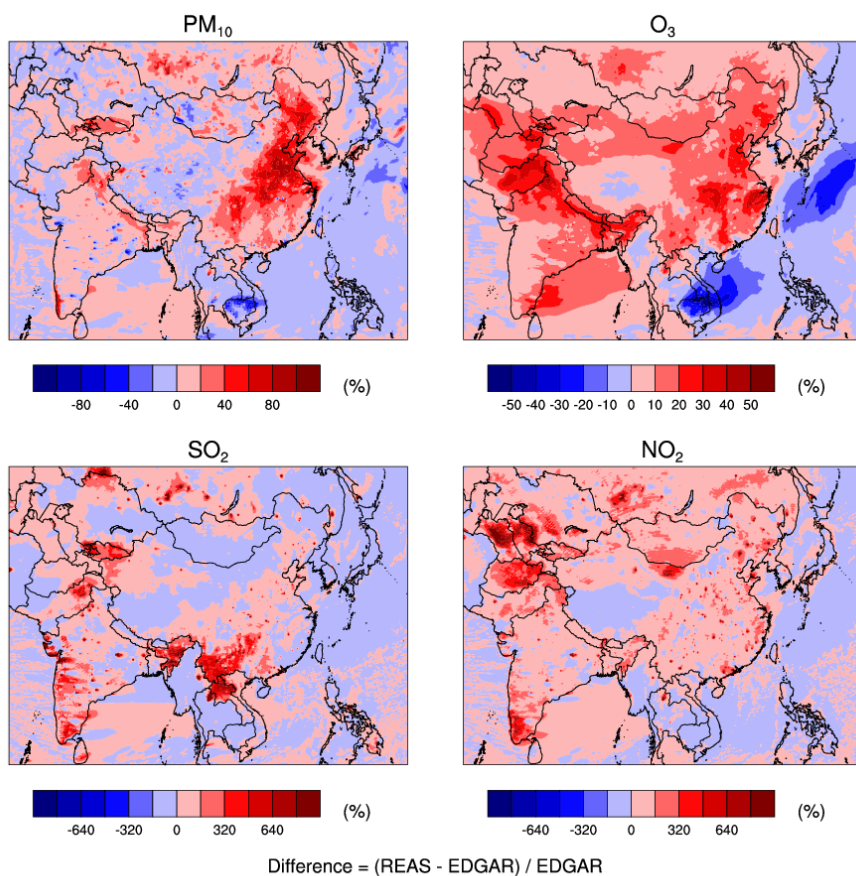
Figure 3. Percentage difference of 14-day mean PM_{10}, O_3, SO_2, and NO_2, between WRF-Chem simulations with REAS emissions (WRF-Chem-REAS) and EDGAR emissions (WRF-Chem-EDGAR).
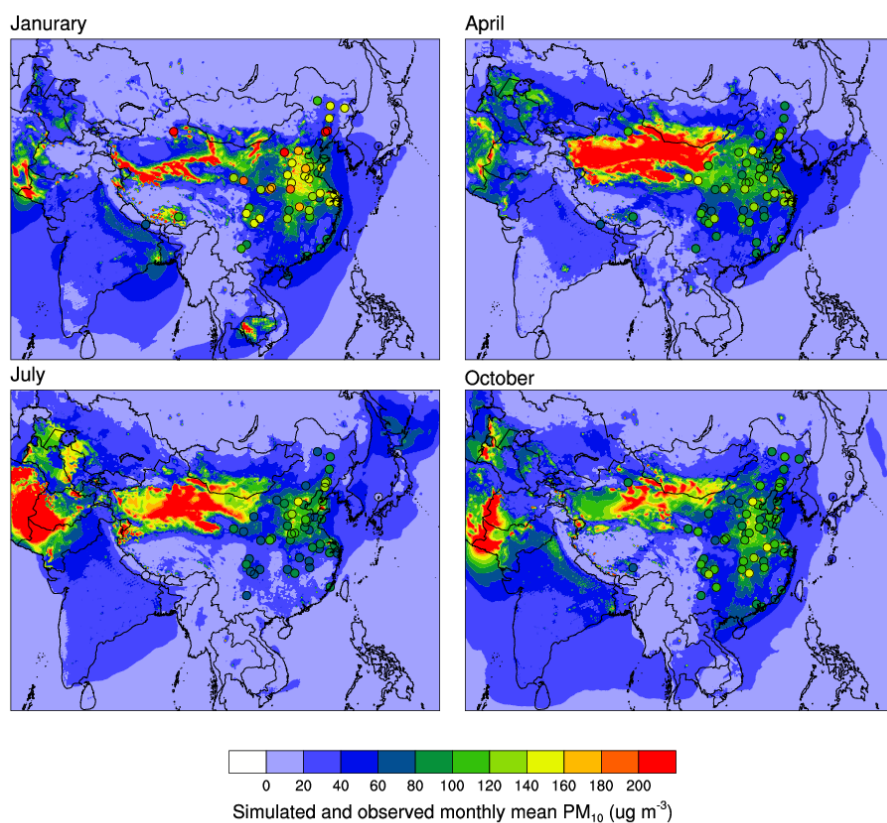
Figure 4. Simulated and observed monthly average surface PM_{10} in 2007 using WRF-Chem-REAS. The filled circles indicate the observed monthly average values.
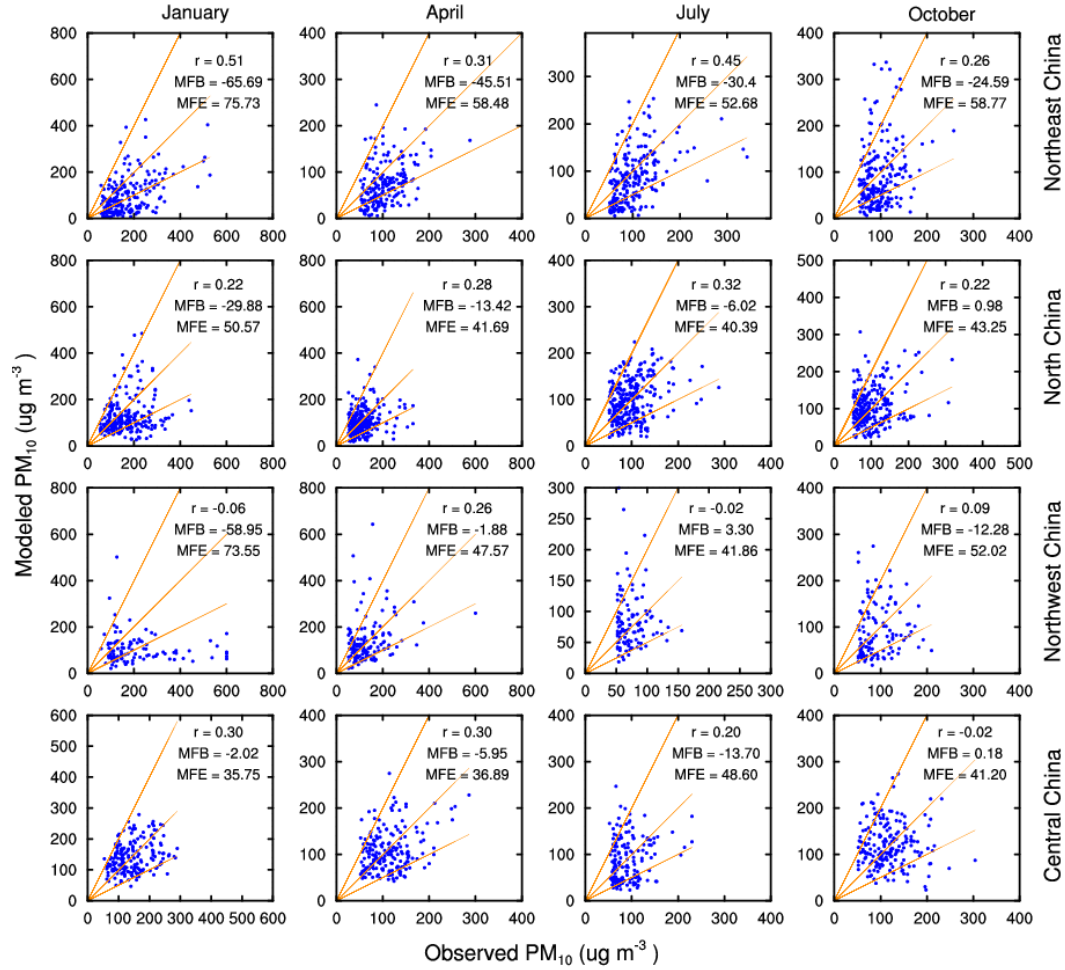
Figure 5. Comparisons of simulated and observed daily mean PM_{10} ($\mu g\ m^{-3}$) at Northeast, North, Northwest, and Central China in each month. The model to observation ratios of 2:1, 1:1, and 1:2 are represented in orange lines. Monthly average performance statistics (r, MFB, and MFE) are listed.

24

Figure 6. Comparisons of simulated and observed daily mean PM_{10} ($\mu g\ m^{-3}$) at East, Southwest, South region in China, and Japan in each month. The model to observation ratios of 2:1, 1:1, and 1:2 are represented in orange lines. Monthly average performance statistics (r, MFB, and MFE) are listed.
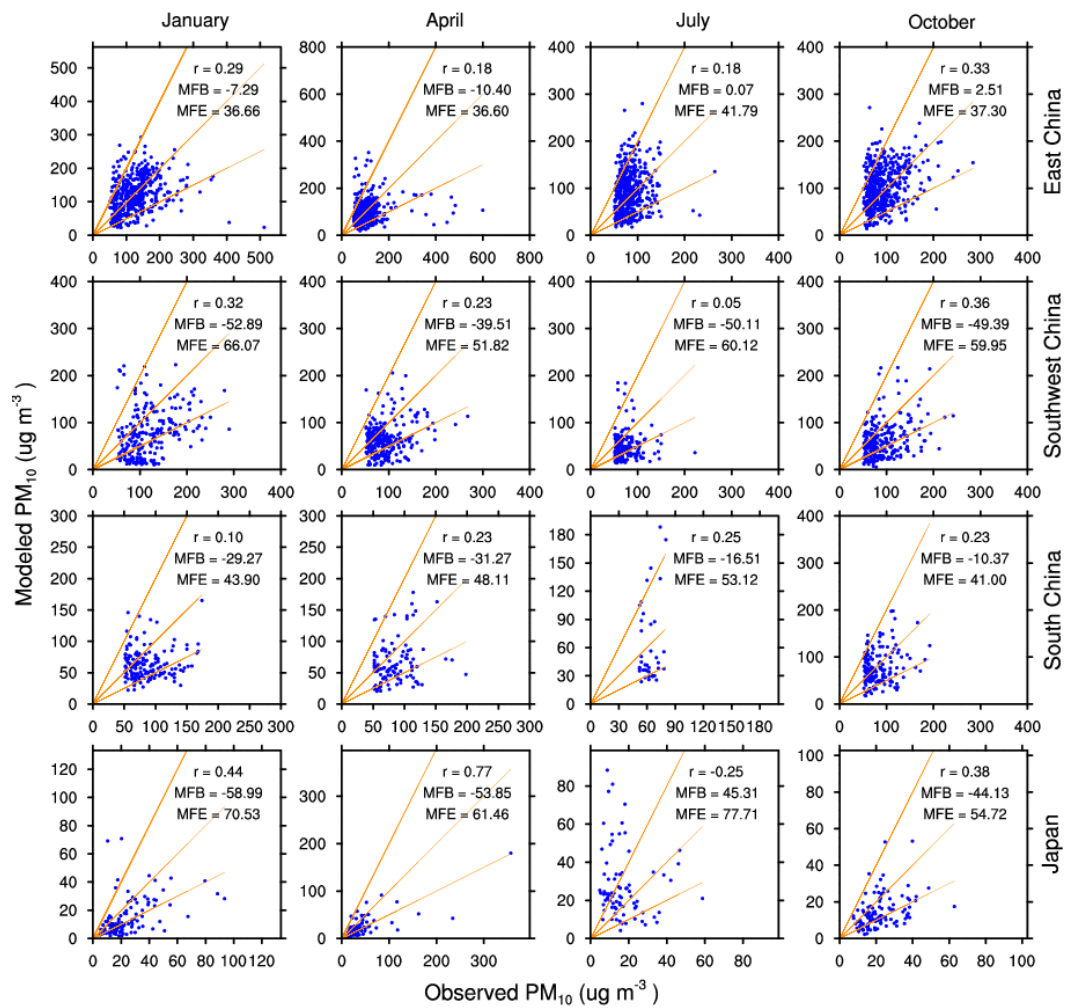
Figure 7. Simulated and observed monthly average surface O_3 in 2007 using WRF-Chem-REAS. The filled circles indicate the observed monthly average values.

Figure 8. Comparisons of observed (blue dots) and modeled (red lines) daily mean O_3 (ppbv) at seven sites in Japan and one site in Taiwan.
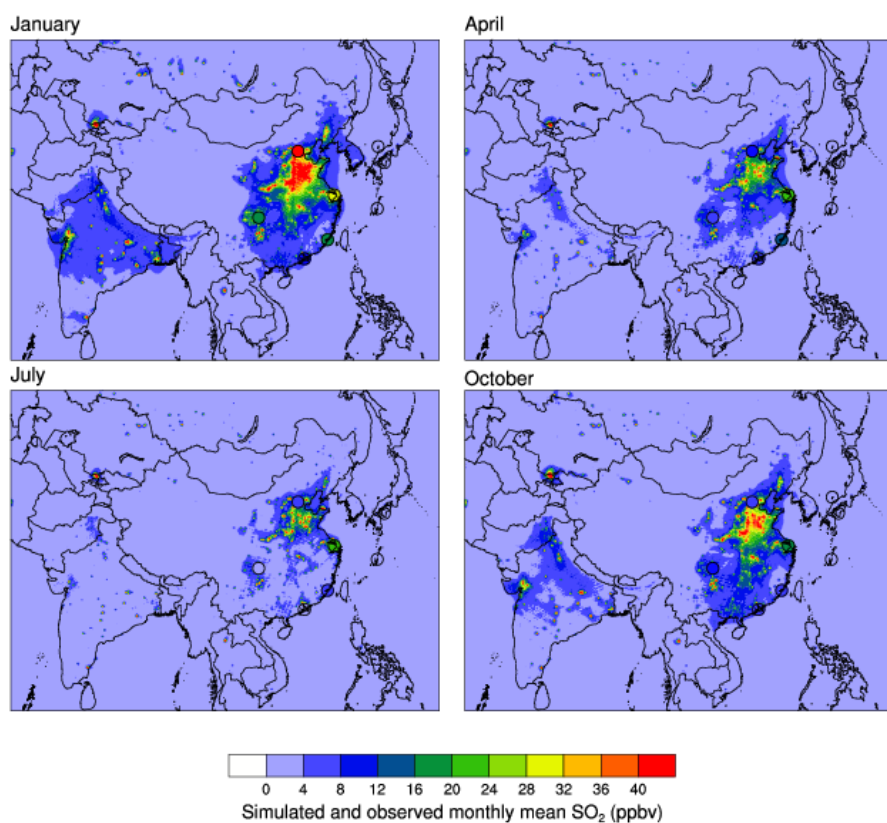
Figure 9. Simulated and observed monthly average surface SO_2 in 2007 using WRF-Chem-REAS. The filled circles indicate the observed monthly average values.
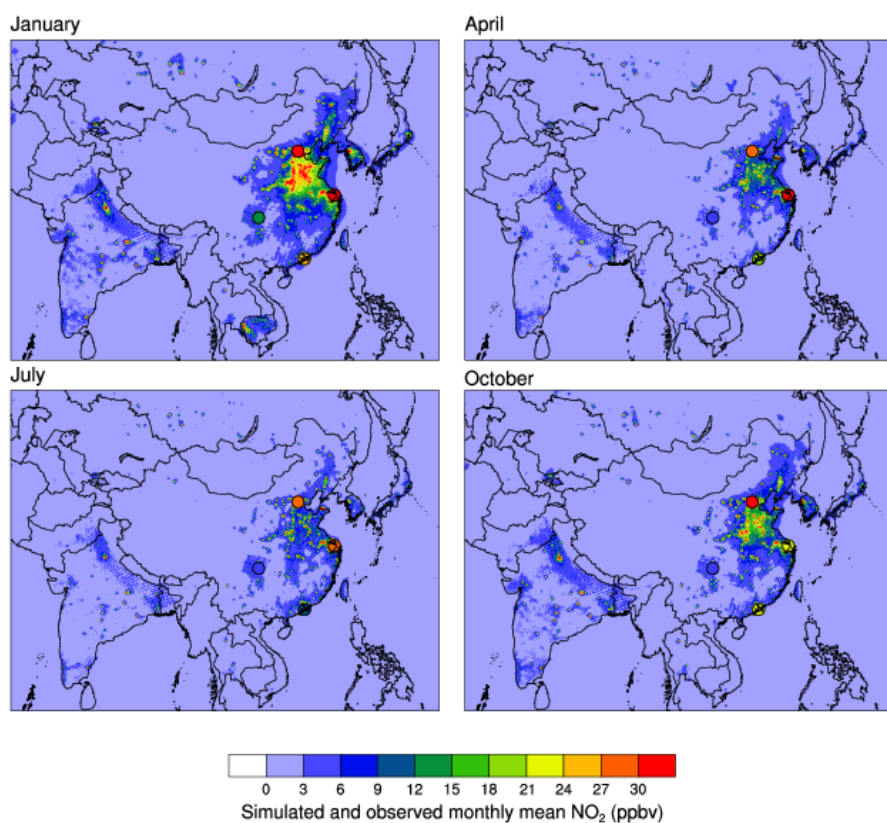
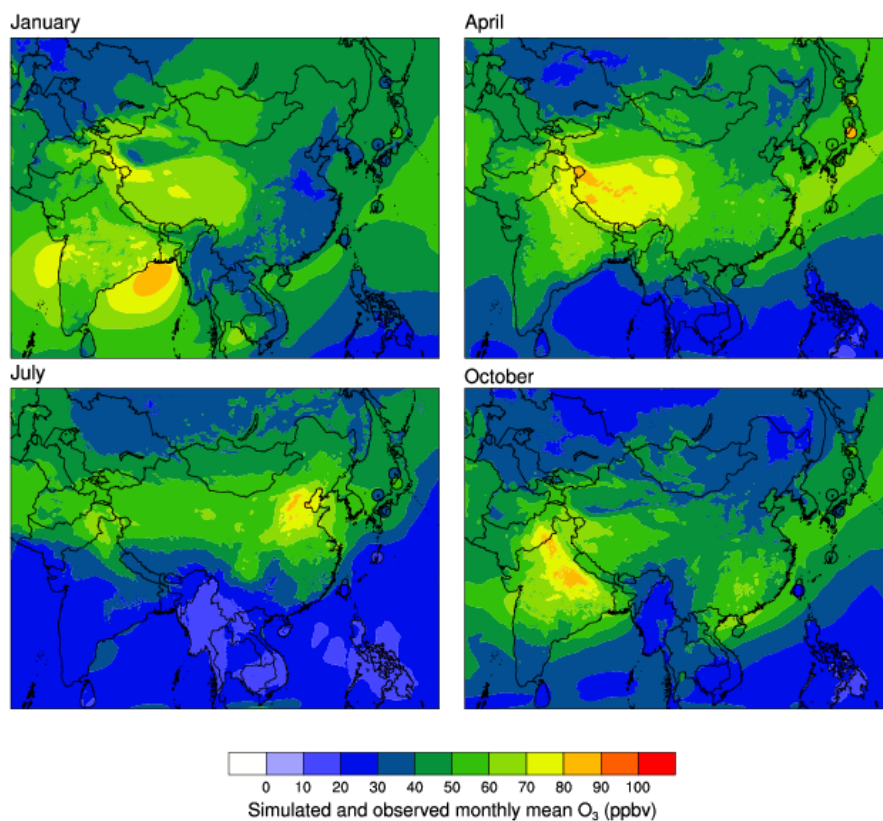**Figure 10.** Simulated and observed monthly average surface NO_2 in 2007 using WRF-Chem-REAS. The filled circles indicate the observed monthly average values.
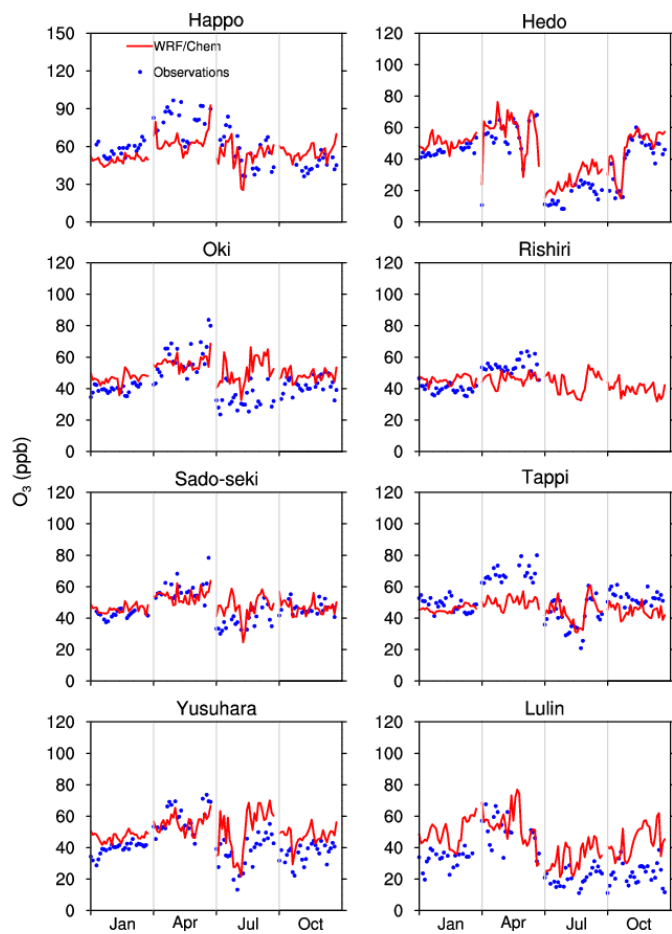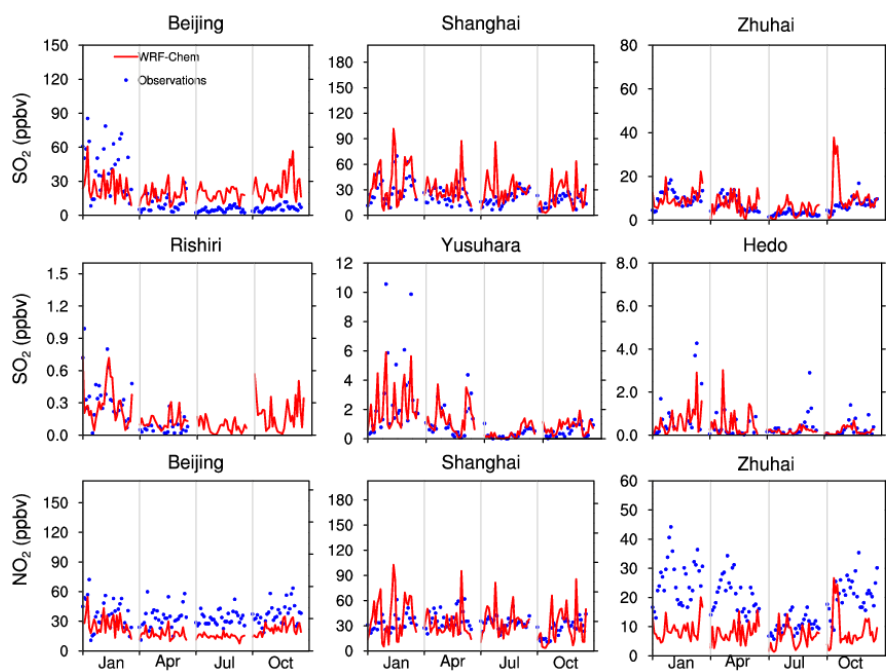
Figure 11. Comparisons of observed (blue dots) and modeled (red lines) daily mean SO_2 (ppbv) at six sites at six sites in China and Japan and NO_2 (ppbv) at three sites in China.

Table 1. List of total emissions for major pollutants from REAS and EDGAR over the model domain in July 2007. Unit is Tg month^{-1}.

Emissions Inventory	PM_{10}	CO	SO_2	NO_x	NMVOCs	NH_3
REAS	2.73	25.05	4.62	4.61	3.67	2.607
EDGAR	3.07	21.25	4.62	3.33	4.56	1.694

Table 2. Statistical measures calculated for model simulations using REAS and EDGAR as emissions inputs for PM_{10}, O_3, SO_2, and NO_2. r is correlation coefficient between observations and model simulations; NMB (%) is the normalized mean bias between observations and model simulations; MFB (%) and MFE (%) are the mean fractional bias and mean fractional error; NMSE is the normalized mean square error between observations and model.

Pollutant	REAS					EDGAR				
	r	NMB	MFB	MFE	NMSE	r	NMB	MFB	MFE	NMSE
PM_{10}	0.38	-2.04	-11.49	46.42	0.36	0.20	-27.28	-37.34	56.70	0.58
O_3	0.83	19.11	24.50	30.95	0.10	0.82	19.20	25.24	32.33	0.10
SO_2	0.72	138.64	51.60	84.93	3.58	0.64	98.42	70.38	94.09	2.03
NO_2	0.68	-18.32	-22.50	50.98	0.41	0.66	-59.88	-71.52	83.05	1.57

Table 3. *Statistical performance of WRF-Chem-REAS simulations for* PM_{10} *in 2007.* Count is the total number of observations for calculation; Obs ($\mu g\ m^{-3}$) and Model ($\mu g\ m^{-3}$) are 4-month mean daily average value of observations and model simulations, respectively. Other indicators and associated units are described in Table 2.

Region	Count	Obs	Model	r	NMB	MFB	MFE	NMSE
Central China	726	117.45	114.21	0.32	-2.75	-5.23	40.47	0.25
East China	1908	103.05	102.41	0.28	-0.63	-3.85	38.05	0.31
North China	1068	116.35	105.35	0.30	-9.45	-11.52	43.65	0.39
Northeast China	826	119.07	87.83	0.39	-26.24	-41.15	61.26	0.59
Northwest China	462	126.86	105.80	0.13	-16.60	-16.54	53.39	0.95
South China	452	82.74	68.97	0.18	-16.64	-22.27	44.68	0.31
Japan	409	25.44	20.83	0.27	-18.10	-32.34	65.24	2.00
Nepal	89	49.63	21.15	0.29	-57.38	-47.89	75.07	2.10
All sites	6874	102.46	89.15	0.39	-12.99	-19.95	48.40	0.46

Table 4. *Statistical performance of WRF-Chem-REAS simulations for* O_3 *in 2007.* The unit of Obs and Model is ppbv. Other statistical indicators and associated units are described in Table 2.

Location	Sites	Count	Obs	Model	r	NMB	MFB	MFE	NMSE
	Happo	81	61.04	55.57	0.55	-8.95	-7.30	20.57	0.06
	Hedo	90	39.59	45.79	0.93	15.68	20.60	22.42	0.04
	Oki	99	43.72	50.19	0.60	14.81	16.01	20.18	0.06
Japan	Rishiri	54	47.14	46.12	0.03	-2.16	-0.92	15.41	0.03
	Sado-seki	82	46.24	47.85	0.61	3.48	4.59	12.13	0.02
	Tappi	101	51.75	45.95	0.56	-11.21	-9.84	17.65	0.05
	Yusuhara	102	42.80	47.68	0.75	11.40	12.75	17.31	0.04
Taiwan	Lulin	94	30.89	44.89	0.62	45.34	41.31	44.05	0.23
All sites		703	45.05	47.98	0.67	6.51	10.48	21.62	0.06

Table 5. *Statistical performance of WRF-Chem-REAS simulations for* SO_2 *in 2007.* The unit of Obs and Model is ppbv. Other statistical indicators and associated units are described in Table 2.

Location	Sites	Count	Obs	Model	r	NMB	MFB	MFE	NMSE
Japan	Happo	65	0.60	0.72	0.53	19.27	20.96	77.56	1.23
	Hedo	86	0.51	0.37	0.66	-27.57	-12.17	69.44	1.70
	Oki	89	0.85	0.82	0.52	-3.60	29.31	69.73	1.77
	Rishiri	50	0.23	0.22	0.71	-2.90	17.84	55.33	0.46
	Tappi	97	0.43	0.37	0.65	-13.66	-1.71	51.61	0.78
	Yusuhara	99	1.27	1.26	0.82	-0.59	26.55	63.58	0.72
China	Xiamen	122	11.79	4.90	0.14	-58.42	-70.79	81.26	1.62
	Jinyunshan	123	10.10	17.81	0.50	76.34	62.19	75.48	0.85
	Zhuhai	123	6.88	8.16	0.29	18.74	5.27	52.50	0.67
	Beijing	123	15.65	21.74	0.32	38.92	63.38	91.86	1.05
	Shanghai	123	22.71	30.57	0.38	34.57	20.10	51.59	0.56
All sites		1100	7.80	8.82	0.64	13.06	8.89	65.80	1.52

Table 6. *Statistical performance of WRF-Chem-REAS simulations for* NO_2 *in 2007.* The unit of Obs and Model is ppbv. Other statistical indicators and associated units are described in Table 2.

Location	Sites	Count	Obs	Model	r	NMB	MFB	MFE	NMSE
China	Beijing	123	32.17	18.63	0.47	-42.09	-53.69	58.67	0.48
	Shanghai	123	29.45	30.57	0.21	3.81	-9.26	46.65	0.41
	Jinyunshan	123	7.04	2.82	0.34	-59.89	-74.42	87.77	2.16
	Zhuhai	123	19.42	7.97	0.11	-58.95	-82.08	86.11	1.34
All sites		492	36.78	15.00	0.56	-31.88	-54.86	69.80	0.69